4.13
Record of Mineral Aerosols and Their Role in the Earth System

K. E. Kohfeld
Simon Fraser University, Burnaby, BC, Canada

and

I. Tegen
Leibniz Institute for Tropospheric Research, Leipzig, Germany

Change begets change … The mine which Time has slowly dug beneath familiar objects is sprung in an instant; and what was rock before, becomes but sand and dust.

Charles Dickens

All we are is dust in the wind, dude.

Ted, Bill and Ted's Excellent Adventure

4.13.1 INTRODUCTION

4.13.1.1 What is Dust?

Soil dust is a type of mineral aerosol, and comprises one component of the total atmospheric aerosol loading. Atmospheric aerosols

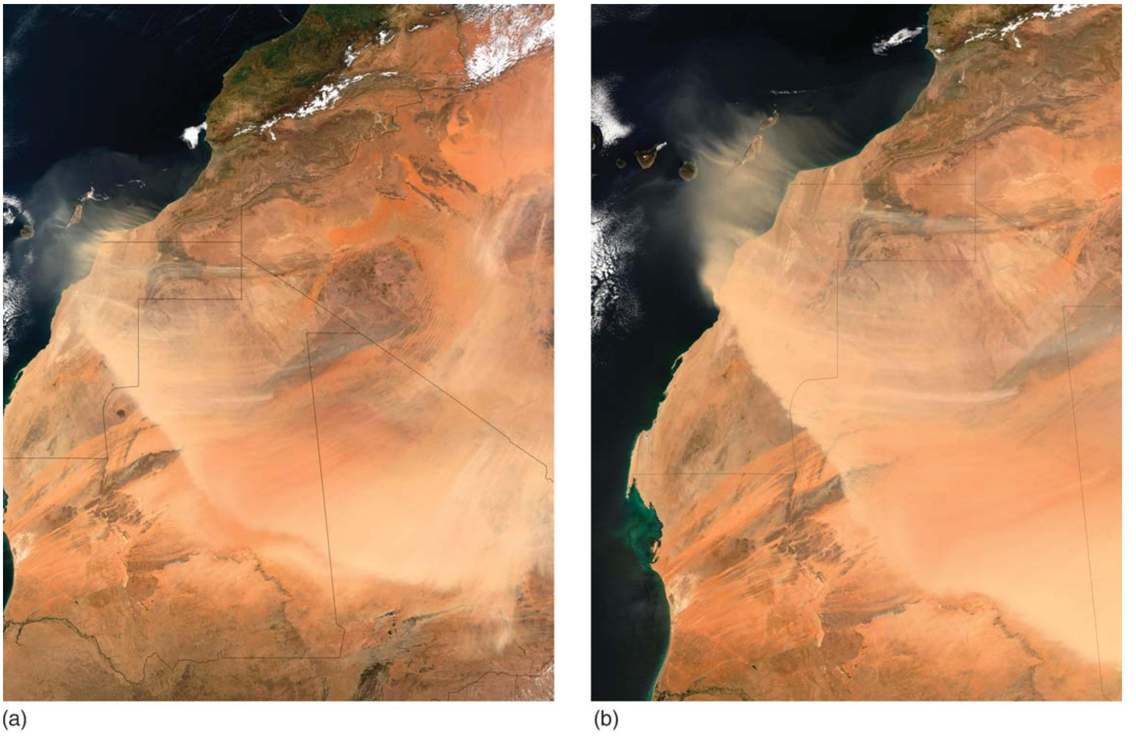

Figure 1 Satellite image of a Saharan dust storm. A long line of Saharan dust swept across Mali, Mauritania, and Western Sahara and out over the Canary Islands on March 3, 2004 when the Moderate Resolution Imaging Spectroradiometer (MODIS) acquired these images during the morning (a) and afternoon (b) passovers. As the day progressed, the dust grew thicker and the storm extended farther west. Image courtesy of the NASA Visible Earth Observatory (Visible Earth, 2006).

play an important role in the climate system, affecting the energy balance of the atmosphere by controlling the amount of radiative energy that enters and exits, through the scattering and absorption of radiation. They can influence important atmospheric processes such as cloud formation, which in turn affect regional energy balances as well as the chemistry (e.g., pH) and quantity of precipitation. The degree to which atmospheric aerosols, both anthropogenic and natural, affect climate remains an important question in earth system science, and has been addressed in Chapter 4.04. For the purpose of this review, we will focus strictly on soil dust and its role within the earth system.

Atmospheric soil dust is defined here as particles that are formed in soils and emitted into the atmosphere during strong surface wind events. Soil dust particles are a combination of irregular-shaped mineral grains such as quartz, feldspars, and calcite, clay minerals rich in elements such as aluminum, and oxides and hydroxides rich in elements such as iron. The composition of dust can change depending on the source region. A compilation by Claquin *et al.* (1999) indicates that quartz is the most abundant mineral in the silt size fraction of the soil (particles in the size range of 2–50 μm diameter), and illite is the most abundant clay mineral. The chemical properties of dust can change during atmospheric transport when dust surfaces become coated with soluble sulfate and nitrate species. Soil particles that are generally $<$60–100 μm in diameter can be picked up by wind, and far-traveled dust is typically around 2 μm in diameter (Seinfeld and Pandis, 1997). Atmospheric soil dust particles are visible in the atmosphere as a haze. High dust aerosol loads originate from dust storms that can reduce atmospheric visibility to $<$1 km and are even visible from space (Figure 1).

4.13.1.2 Why is Dust Important?

Atmospheric dust can have substantial regional impacts on agriculture and human health. Dust storms affect agriculture through extensive erosion of the soil surface (Nordstrom and Hotta, 2004). Dust can also affect the quality of the air that we breathe. Minute particles of soil dust with diameters smaller than 10 μm (PM10) in the atmosphere have been shown to be damaging to human respiratory health (Chapter 9.07). Furthermore, certain toxic metals, such as mercury and arsenic, can be associated with the transport of aeolian dust (Gill *et al.*, 2002; Cannon *et al.*, 2003; Givelet *et al.*, 2004).

Although there have been efforts to quantify the interactions between atmospheric dust and regional climate (e.g., Seinfeld *et al.*, 2004; House *et al.*, 2006), the overall radiative impact of soil dust on the climate cycle is still not well quantified. In fact, it is not known if soil dust aerosols on the whole will have a net warming or cooling effect (Houghton *et al.*, 2001). Dust can either increase or decrease planetary albedo, depending on both the single scattering albedo of the dust particle as well as the albedo of the underlying surface. For example, dust over optically ''dark'' regions, such as oceans or forests, can have a cooling effect (see, e.g., Tegen *et al.*, 1996). Alternatively, dust can increase the absorption of solar radiation over high reflective regions such as ice sheets, snow, or even desert surfaces. The role of dust as condensation nuclei in cloud formation and precipitation is unknown but potentially important (e.g., Rosenfeld *et al.*, 2001; Levin *et al.*, 2005). The radiative forcing of high atmospheric dust concentrations in the geologic past have been proposed as a means of cooling the tropics (Claquin *et al.*, 2003) and the midcontinental United States (Roberts *et al.*, 2003), but also as a means of accelerating deglaciation (Overpeck *et al.*, 1996).

Dust can also impact the earth system via biogeochemical feedbacks (see Section 4.13.7.2). Soil dust contains micronutrients (such as iron, zinc, and cadmium) and macronutrients (such as phosphate and silica) all of which can fertilize terrestrial and marine ecosystems. Iron in particular has been suggested to limit phytoplankton growth in ocean regions, which are otherwise rich in macronutrients, such as nitrate (Martin and Fitzwater, 1988). As such, changes in dust inputs to the ocean could affect marine productivity as well as the sequestration of carbon in the deep sea (Martin, 1990).

Assessing the magnitude of these regional impacts, radiative forcing, and biogeochemical feedbacks in the earth system requires an ability to quantify the amounts of dust produced, both in the past and in the present. Predicting future changes in the dust cycle and its interaction with climate are even more uncertain. Estimating the importance of dust depends on our ability to estimate (1) the natural processes controlling dust entrainment, transport, and deposition; (2) changes in these natural processes due to global and regional climate change; and (3) changes in dust production due to human impacts on land use. Our ability to simulate these processes requires correct parameterization of these processes as well as data to constrain them.

The purpose of the chapter is to review the current knowledge about the record of mineral aerosols. This chapter will first review the main processes of the dust cycle—entrainment, transport, and deposition (Section 4.13.1.3). The tools and records used to measure changes in entrainment, transport, and deposition of dust in the geologic past will be discussed in Section 4.13.2, followed by an elaboration of how dust has varied through geologic history (Section 4.13.3). We follow with parallel discussions of how soil dust processes are measured for the modern climate (Section 4.13.4), and what these measurements have revealed with regard to recent variability in the dust cycle (Section 4.13.5). We proceed by explaining how data are used to inform models of the dust cycle (Section 4.13.6), and summarize what is currently known about the radiative and biogeochemical feedbacks of atmospheric dust within the earth system (Section 4.13.7). We conclude with a future outlook of important questions that still need to be addressed in the field of dust research (Section 4.13.8).

4.13.1.3 Dust Cycle Processes: Entrainment, Transport, and Deposition

Most atmospheric dust has its origin in arid to semi-arid regions of the Earth and is emitted from regions that are sparsely vegetated (i.e., $\lesssim$15% vegetation cover). Today, most dust is produced in deserts of northern Africa (Sahara, Sahel) and the Middle Eastern regions (Figure 2), contributing up to 70% to the modern global annual dust emission fluxes (Jickells *et al.*, 2005). Other sources of importance include the desert regions of Asia and Australia.

In regions where the soil is exposed and the soils contain fine and loose particles, winds are able to lift soil particles into the air. The dependence of the dust flux F on the surface wind friction velocity u^* can be written for a given particle size as

$$F \propto u^{3*}\left[\left(1+\frac{u^*_{\mathrm{tr}}}{u^*}\right)\left(1-\frac{u^{2*}_{\mathrm{tr}}}{u^{2*}}\right)\right] \quad \text{for } u^* > u^*_{\mathrm{tr}}$$

with the friction velocity and u^*_{tr} the threshold friction velocity (Marticorena and Bergametti, 1995). Surface wind friction velocities are computed from surface wind speeds and surface roughness data, assuming neutral stability conditions, as $u^* = u(z)\kappa/\mathrm{In}(z/z_0)$, where u is the surface wind speed at reference height z, κ is the von Karman constant, and z_0 is the

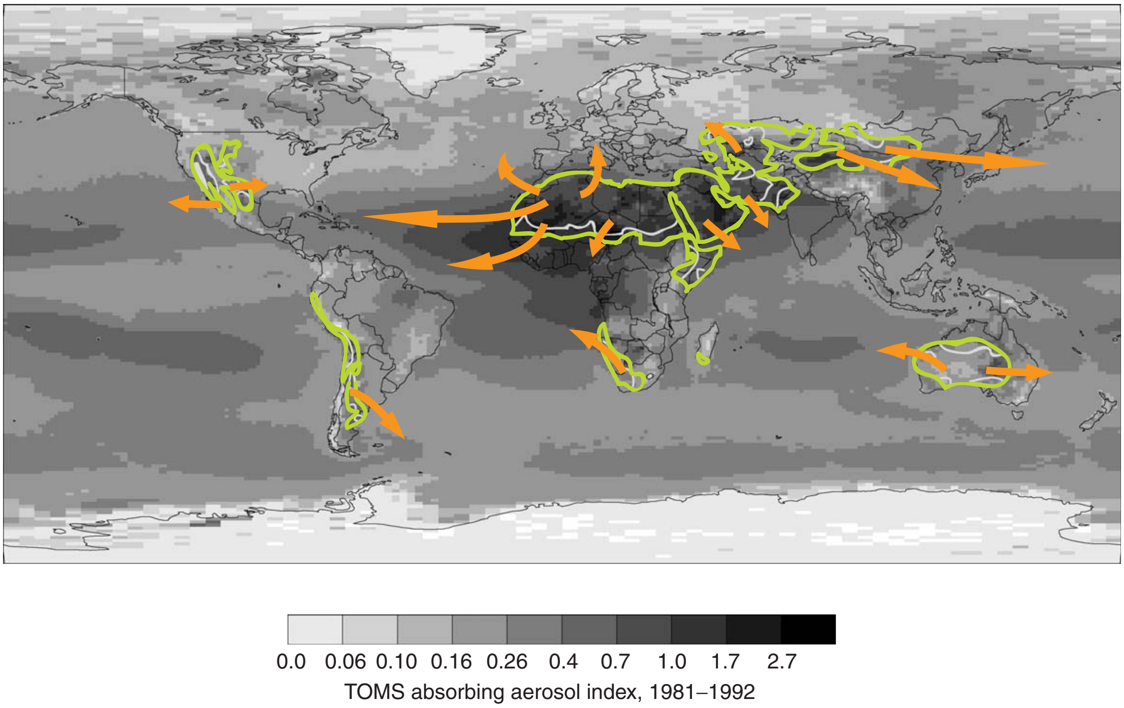

Figure 2 TOMS aerosol index values averaged from 1981 to 1992. Largest source areas are located in arid tropical–subtropical regions of Africa and the Middle East. Green lines outline regions that are considered dust sources. Orange arrows indicate the general direction of dust transport from these regions.

aerodynamic roughness length. The minimum wind friction velocity u^*_{tr} required to lift soil particles is called the "threshold wind velocity" and depends on a combination of soil texture, moisture, and the surface roughness. Silt-sized (2–50 μm diameter) or fine sand (50–250 μm diameter) particles are the easiest to lift and require the lowest surface wind speeds to become airborne, while larger particles are heavier and have higher threshold wind velocities. The smallest, clay-sized particles (diameter <2 μm) have a greater surface area-to-volume ratio when compared with silt-sized particles. These clay-sized particles tend to adhere to each other by cohesive forces (van der Waals forces and electrostatic charges (Iversen and White, 1982), and thus cannot be lifted directly from the ground as individual particles. Soils containing more than 20% clay-sized particles are considered to be only weak emitters of dust aerosols (Gillette, 1979; Marticorena and Bergametti, 1995). Soil particles with diameters of 2 μm or less, which can be transported by winds over large distances, are usually dislocated from soil aggegates at the soil surface through the impact of saltating sand grains (e.g., Lu and Shao, 1999).

Within the deserts, certain regions represent "hot spots" of dust production, emitting higher amounts of dust compared with other desert areas. These regions containing large amounts of fine and loose soil particles that can form dust aerosols are referred to as preferential dust sources (Gillette, 1999; Ginoux *et al.*, 2001; Prospero *et al.*, 2002; Tegen *et al.*, 2002; Tegen, 2003). Typically, dried paleolake beds such as the Bodele depression in Chad or the Lake Eyre basin in Australia, playa sediments, or alluvial fans can be "hot spot" dust sources (Pye, 1987). For example, the Bodele depression contains the most active dust source worldwide (Prospero *et al.*, 2002). There, dust emission occurs from massive diatomite sediments that formed 6,000 years ago when the basin was covered by the paleolake Mega-Chad (Washington *et al.*, 2006).

Estimating global annual dust emissions is complicated because we do not have observational datasets that are extensive and detailed enough to quantify dust emissions on a global scale (see Cakmur *et al.*, 2006 for a study of using various datasets to constrain emissions). Currently, emissions are generally calculated using global dust models, but uncertainties are introduced from model treatments of land-surface characteristics, the parameterizations controlling the mobilization of dust, and the controlling meteorological factors. As a result, current estimates of dust emissions span a large range, between 1,000 and 2,500 Tg (10^{12} g) of dust emitted globally each year (Zender *et al.*, 2004).

Our knowledge of the atmospheric burden, or the amount of dust that remains in the atmosphere at any one time, is even less concise than our knowledge of emissions, and varies by a factor of 4. The values range from 8 to 36 Tg (Zender *et al.*, 2004), with uncertainty resulting from observational uncertainties as well as a difficulty constraining what controls the removal of dust from the atmosphere, or deposition. The removal of dust from the atmosphere occurs through two processes known as "wet" or "dry" deposition. During dry deposition, airborne particles fall to the ground by gravitational settling (where the settling velocity depends on the square of the particle diameter), and mixing to the surface by turbulent air motions. As a consequence of the gravitational settling, large particles (with diameters greater than $\sim 5\,\mu m$) are removed from the air rather close to their source of entrainment, but finer particles remain suspended in the atmosphere and can be transported long distances. As a result, areas of deposition that are remote from dust source areas (such as the polar ice caps) are dominated by fine particles with sizes on the order of $1–2\,\mu m$. During wet deposition, dust is scavenged by precipitation droplets and rained out of the atmosphere. Highest rates of dust deposition are found directly downwind of the largest dust sources such as the Sahara and Sahel desert regions of North Africa. These large dust fluxes are not surprising because the largest particles are removed from the air near the source. The fine dust from North Africa can be transported across the tropical Atlantic and reach as far as the Amazon basin. Other areas of high deposition are associated with the deserts of central Asia. When transported within higher atmospheric layers at several kilometers altitude, soil particles from Asian dust storms occurring in spring can be transported as far as North America and Greenland, and in some cases, Europe (Grousset *et al.*, 2003). Less-extensive dust sources in Australia, southern Africa, and Patagonia have a more local influence on dust deposition (Duce *et al.*, 1991). Regions that are far from any major sources of dust, such as Greenland and Antarctica (Figure 2), are characterized by extremely low dust deposition (Figure 3a).

4.13.2 GEOLOGIC RECORDS OF DUST: PALEOENVIRONMENTS AND TOOLS

4.13.2.1 Paleoenvironments

The factors controlling the dust cycle—aridity, vegetation cover, winds, and precipitation—are all related to climatological factors. Thus, it is not surprising that dust emissions, transport, and deposition have changed with climate on geological timescales, and will change over future timescales as well. In fact, the geologic record of dust provides a rich history of climate cycles, as archived on the land (through terrestrial loess deposits and lake sediments), in the ocean (via marine sediments), and in remote polar areas (from ice cores).

The geologic record of dust is by nature a record of "deposition," stored in several different paleoenvironments. Geological deposits of dust are found on all parts of the globe, at the bottom of lakes and also as sedimentary sequences on land called "loess" (Pye, 1987, 1995). Loess deposits are present on every continent and are composed of wind-blown, silt-sized dust particles ($2–50\,\mu m$) that are generally found very near to dust source regions because of their relatively large sizes. Although some "desert loess" is found in subtropical arid regions downwind of arid sources (e.g., Smalley and Krinsley, 1978), much loess is found near glaciogenic source regions, where materials have been ground up by glacial activity and then transported by rivers to areas that are relatively arid and free of vegetation (Smalley and Smalley, 1983). Largest thicknesses of loess began to accumulate on the continents over the last 2.8 Myr, likely associated with the climate changes associated with glacial–interglacial cycles (Derbyshire, 2003).

Aeolian materials are also found in lake and marine sediments (for full review see Kohfeld and Harrison, 2001). In general, the aeolian materials archived in marine sediments are located further from dust source regions and so, with rare exception, are composed of smaller grain size material, and in lesser abundances compared with lake sediments. The advantage of lake and marine sedimentary archives is that the records tend to be more continuous than terrestrial records, and therefore can provide an uninterrupted record of changes in dust deposition through geologic time. Furthermore, these sediments provide more direct information about the inputs to lacustrine and marine ecosystems, which may be important when considering biogeochemical feedbacks of dust. There are, however, some disadvantages to these records. For example, the extraction of aeolian signals is sometimes more complicated because of the influence of detritus from rivers and ice rafting, as well as sediment winnowing or resuspension processes (Rea, 1994). Sediment records can also be affected by mixing due to bioturbation, and this process can make it difficult to determine abrupt changes in dust deposition when sedimentation rates are low (see, e.g.,

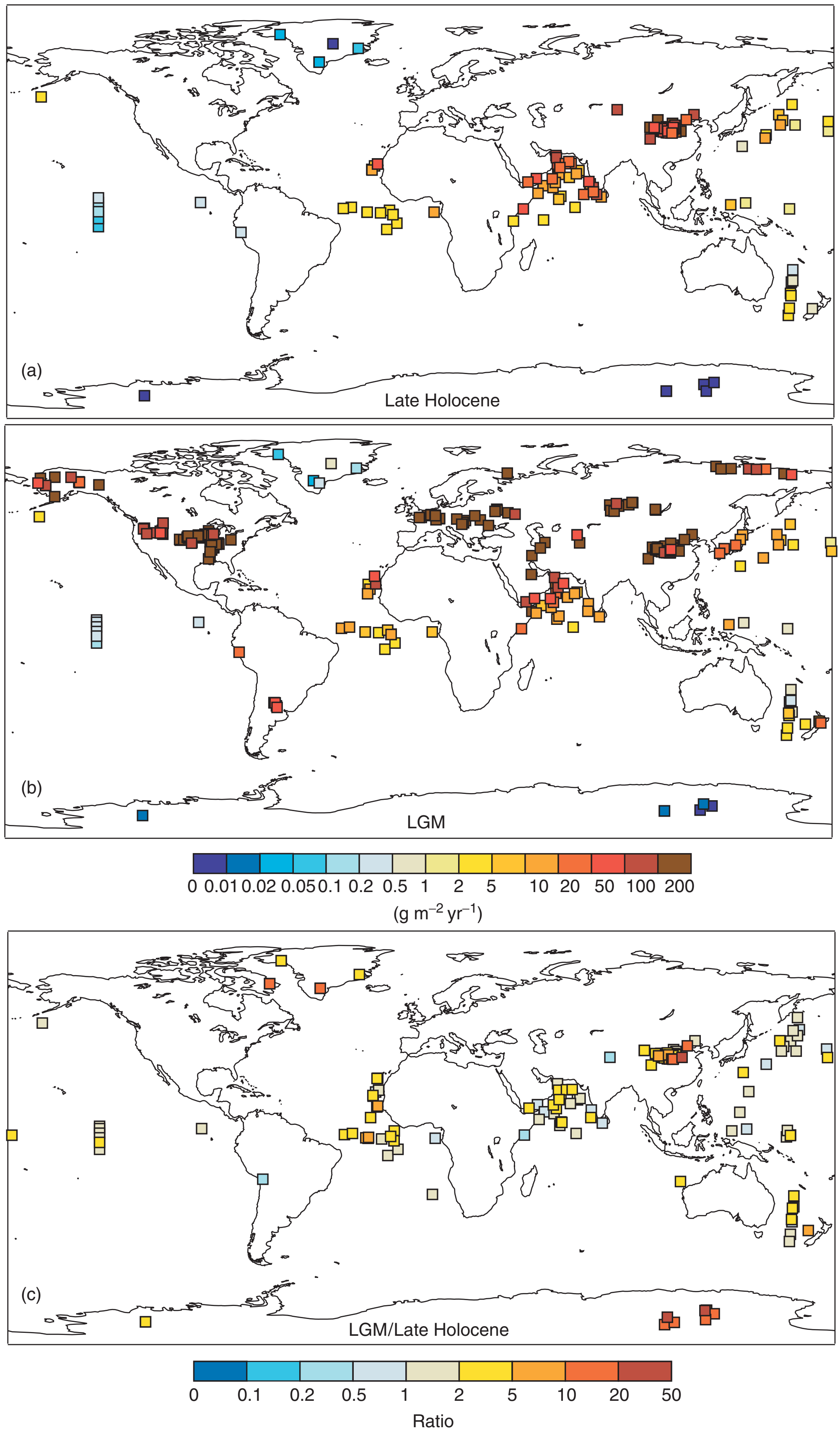
(a)
Late Holocene
(b)
LGM
0 0.01 0.02 0.05 0.1 0.2 0.5 1 2 5 10 20 50 100 200
(g m^{-2} yr^{-1})
(c)
LGM/Late Holocene
0 0.1 0.2 0.5 1 2 5 10 20 50
Ratio

discussion from Ruddiman, 1997). Finally, unlike loess deposits, marine and lacustrine sediments are not 100% aeolian, butff are generally dominated by biogenic materials such as carbonate and opal. One standard procedure for isolating the terrigenous fluxes is by determining the differences between the total fluxes and the biogenic components. This differencing procedure produces large uncertainties, in particular when fluxes of terrigenous materials are very low. One promising means of getting around the dilution effects is to use trace elements, such as ^{232}Th, which are enriched in continental crust material and therefore can serve as more direct geochemical tracers of dust (e.g., Anderson *et al.*, 2006). In spite of these issues, ocean sediments make up the majority of the Quaternary archive of long-distance transported dust, and can be useful for providing a first-order indication of deposition changes in mineral soil dust over longer timescales.

Glaciers and ice sheets also serve as collectors of atmospheric dust that is transported and deposited directly onto the ice and/or snow surface. Dust either settles or is rained out and is directly incorporated into the ice and is disturbed by fewer postdepositional problems compared with other depositional regimes. With the exception of some tropical glaciers, the aeolian material that has been retrieved from ice cores tends to be long distances from dust sources.

4.13.2.2 Dust Deposition

The mass accumulation rates (MAR) of dust are determined in the following manner:

$$\mathrm{MAR} = \mathrm{LSR} \times \mathrm{DBD} \times f$$

where LSR is the linear sedimentation rate ($\mathrm{m\,yr^{-1}}$), DBD the bulk density of the sediment ($\mathrm{g\,m^{-3}}$), and f the fraction of the sediment that is considered aeolian. Some variant on this equation is necessary for measuring a mass accumulation rate no matter what the paleoenvironment (see Kohfeld and Harrison, 2001).

In ice cores, information regarding the fraction of wet versus dry deposition has sometimes been inferred by combining both simple and complex precipitation models with additional information about precipitation rates and snowfall (Alley *et al.*, 1995; Werner *et al.*, 2003). In general, however, changes in the mass accumulation rates of dust provide us with a combined picture of the overall changes in the intensity of the dust cycle, integrating aspects of source, transport, and deposition.

4.13.2.3 Dust Sources and Emissions

While changes in deposition rates do not give a direct measure of dust emissions and transport, the deposited archive can provide us with some clues through factors such as grain size, mineralogy, and isotopic characterization. Clay mineralogy and isotopic characterization has frequently been used as a means of determining the general location of dust source areas. The changes in grain size of the deposited dust can reflect a combination of distance from source, wind strength as well as deposition regime.

4.13.2.3.1 Geochemical fingerprinting

Dust that enters the atmosphere carries with it a distinct geochemical fingerprint, a signature defined by its clay mineralogy, elemental composition, and isotopic signature. One assumption is that the chemical characteristics of suspended and deposited dust can be used as a means of tracing its origin to the original, parent soil from which it was formed (for review see Grousset and Biscaye, 2005). Provenance is determined by comparing the chemical signatures of dust with the signature of potential source rocks. Source rocks can include both primary sources, which are parent rock materials, or secondary sources, which are a mixture of particles that have already been transported by aeolian or fluvial processes. This method of identifying source regions requires extensive sampling of potential source areas of dust from around the world, and requires that the distinct geochemical signature of the airborne dust is not altered during transport, perhaps via chemical alteration in clouds, or as a result of fractionation during wet deposition.

The clay mineralogy is thought to reflect the parent rock material, drainage, climate, and the degree of physical or chemical weathering. For example, kaolinite is formed primarily through chemical weathering from feldspars and micas, at warm temperatures, and therefore at lower

Figure 3 Mass accumulation rates of dust for the (a) late Holocene period, (b) the Last Glacial period, and (c) the ratio between them. Squares represent estimates from sediment records. Squares in (a) represent values from modern marine sediment traps. Data are derived from the DIRTMAP database (Kohfeld and Harrison, 2001), with additional data from Delmonte *et al.* (2002, 2004a, b), Anderson *et al.* (2006) and Mahowald *et al.* (2006).

latitudes. Alternatively, chlorite is found in soils from cold, high-latitude regions where physical-weathering processes dominate. As a result, the ratio between these two clay minerals in dust provides a first-order indicator of the location of a dust source region (Biscaye, 1965; Biscaye *et al.*, 1997).

In the mid-continental United States, a combination of clay mineralogy and grain size patterns has been used successfully to trace the source regions for loess deposition in Colorado and Iowa (Aleinikoff *et al.*, 1999; Muhs *et al.*, 1999; Muhs and Bettis, 2000; Muhs and Benedict, 2006). Loess is typically associated with areas close to rivers that drained the Laurentide Ice Sheet, but it is also distributed widely over the central Great Plains of Nebraska, Kansas, and Colorado. Geochemical analyses (e.g., concentrations of K_2O, Rb, TiO_2, and Zr) of the Peorian Loess in western Iowa indicate that this aeolian material was likely derived directly from the Missouri River Valley during some periods, and also from regions west of the Missouri River in eastern Nebraska during the latter stages of deposition (Muhs and Bettis, 2000). Analyses of the trace elements Ti, Nb, Zr, Ce, and Y on silts found in the soils in the Colorado Front Range (Muhs and Benedict, 2006) indicate that some portions of these soils are not derived from the parent rocks just below, but rather are aeolian in nature and must have been transported from a more western basin during the early-to-mid Holocene Period (Muhs and Benedict, 2006).

In places where clay mineralogy is not sufficient for determining a unique source, natural and radiogenic isotope tracers can be used to track the different parent lithologies of the source areas (for a recent review, see Grousset and Biscaye, 2005). The isotopic ratios of Sr ($^{87}Sr/^{86}Sr$), Nd ($^{143}Nd/^{144}Nd$), and Pb ($^{206}Pb/^{207}Pb$) have been used extensively to detect provenance in the mid-continental United States (Aleinikoff *et al.*, 1999), in the North Pacific Ocean (Pettke *et al.*, 2000), off Africa (Grousset *et al.*, 1998), in Antarctica (Basile *et al.*, 1997; Delmonte *et al.*, 2004a, b), and Greenland (Biscaye *et al.*, 1997; Svensson *et al.*, 2000; Bory *et al.*, 2002, 2003a, b). These radiogenic isotopes are particularly effective because of the range of isotopic values found between relatively young, volcanic rocks, radiogenically older, crustal-derived materials, and parent soils that comprise a mixture of the two. Used together, the isotope signatures of Sr, Nd, and Pb can help one to discriminate between different aeolian sources.

The use of isotopic fingerprinting has been particularly effective in identifying the sources of dust deposited at the polar ice caps. In Antarctica, the Sr and Nd isotope signatures of dust have demonstrated that southern South America, New Zealand, and regions of the Antarctic Dry Valleys might all serve as sources to the Vostok and EPICA Dome C ice cores (Delmonte *et al.*, 2004a). However, the authors use the small size of the latter two source areas plus the glacial circulation to reason that southern South America remains the most likely source of dust. In Greenland, several studies have used clay mineralogy, Sr, Nd, and Pb isotopes to pinpoint Asian deserts as the source of dust both during cold stadial and warm interstadial periods based on the isotopic characterization of the dust (Biscaye *et al.*, 1997; Svensson *et al.*, 2000).

4.13.2.3.2 Grain size indicators

The grain size distribution of deposited dust is frequently used in paleoclimate studies as an indicator of distance of deposited dust from the dust source, changes in wind strength that carries dust particles, or some combination of the two. Distance-related sorting of dust particles is simply illustrated by the grain size distributions of deposited dust from different paleoenvironments. Near-source sedimentary deposits such as loess are relatively coarse-grained with diameters of 20–60 μm (see, e.g., Muhs and Bettis, 2003). In contrast, dust diameters in marine sediments located at a further distance from source areas range from 0 to 8 μm (Rea, 1994). Aeolian deposits from the Greenland ice cores, that are located large distances from source areas, have grain size distributions ranging from 0.4 to 2.0 μm (Steffensen, 1997). Modal grain sizes range from 1.7 to 2.3 μm in diameter in Antarctic cores, with maximum sizes smaller than 5 μm (Delmonte *et al.*, 2004b).

The relationship between the mean grain size of particles and carrying capacity of wind associated with wind strength has been demonstrated using aeolian sediments collected in sediment traps in the Indian Ocean (Clemens, 1998), where strong positive correlations are observed among median grain size, overlying wind speed, and regional pressure gradients. Long-term trends in aeolian grain size in Indian Ocean marine sediments show a decreasing trend between 3.0 Ma until today, which Clemens (1998) interprets to indicate a steady decrease in the intensity of the winds associated with the southwest monsoon. At great distances from source areas in Greenland and Antarctica, changes in the strength of the wind-carrying sediments have often been inferred from changes in sediment grain size. The mean grain size diameters from Greenland ice cores have been shown to increase during cold, stadial periods (e.g., the Younger Dryas or Last Glacial Periods), in comparison with relatively warmer periods such as the early-to-late Holocene (Steffensen, 1997; Zielinski and Mershon, 1997). These grain size increases are correlative with substantial increases in dust deposition and suggest a possible enhancement of wind intensities during the colder climatic periods.

Grain size distributions of dust in ice cores are not always simply related to changes in wind speed and can also result from changes in the transit time of dust. Recent analyses from the EPICA Dome C core in Antarctic have shown finer grain sizes at the last glacial period compared with data from the Holocene (Delmonte *et al.*, 2002), in contrast to results from other east Antarctic cores (Thompson, 1977; Petit *et al.*, 1981; Briat *et al.*, 1982; De Angelis *et al.*, 1984). Although the dust isotopic signature suggests that the dust at these cores share a common provenance, Delmonte *et al.* (2004a) propose that the finer-grained dust at the EPICA Dome C site was transported via high-altitude air masses that resulted in a longer transit time than for dust at the other Antarctic sites.

In actuality, the grain size distribution of atmospheric dust particles can be affected by several additional factors, including the grain size distribution of soils at the source area, the deflation process, the nature of the deposition, and postdepositional changes. For example, higher surface wind speeds can cause saltating soil particles to dislocate smaller dust particles compared with lower wind speeds. This occurs because the high kinetic energy of saltating particles overcomes the binding energies of clay aggregates (as shown in experimental studies by Alfaro *et al.*, 1998). Higher surface wind speeds in source areas thus can cause enhanced dislocation of both smaller and larger particles compared with particle sizes dislocated at lower wind speeds (Grini and Zender, 2004; Alfaro *et al.*, 1998; Marticorena and Bergametti, 1995). This effect should be taken into consideration for interpreting the particle size information in aeolian sediments.

The nature of the deposition process can also strongly influence the grain size distribution that is recorded. In the atmosphere, the relative contributions of wet versus dry deposition can also affect the grain size distribution of the dust deposited (e.g., Gillette *et al.*, 1974; Johnson, 1979). Studies in Australia have shown that the dust deposited by dry deposition has a unimodal grain size distribution centered around 12–13 μm (Hesse and McTainsh, 1999). In contrast, indiscriminate scavenging of all particle sizes occurs during rainfall events, which results in the observed bimodal distribution of deposited dust, with peaks centered at 3 and 10.5 μm (Hesse and McTainsh, 1999). Once dust has entered the ocean, hemipelagic contamination from river plumes, ice rafting, and turbidites, and bottom water currents can completely alter the sediment grain size distribution (e.g., Rea, 1994). Thus, caution must be exercised in interpreting grain size distributions because deciphering a single cause of changes in grain sizes is not always straightforward.

4.13.3 GEOLOGIC VARIABILITY OF THE DUST CYCLE

What changes have been observed over millions of years; what do we know about the regular "cycles" of dust; and what detailed information about the dust cycle can we reconstruct about the last glacial period? The geologic record of dust has provided a wealth of information about changes in dust relative to past climates.

4.13.3.1 Dust over Long Time Periods

Terrestrial loess deposits and marine sediments both provide important information about the changes in atmospheric dust activity over the last 12 Myr (Pettke *et al.*, 2000), associated with the uplift of the Tibetan Plateau. The longest aeolian sequences on land are from the Chinese Loess Plateau. These loess–paleosol sequences provide a relatively continuous record of changes in moist and arid conditions associated with fluctuations in the East Asian monsoon over the last 2.6 Myr (see, e.g., An, 2000), and more recent evidence suggests that the underlying Red Clay sequence is also aeolian (Zheng *et al.*, 1992; Ding *et al.*, 1998; Guo *et al.*, 2001), dating to as early as 8.35 Ma (Qiang *et al.*, 2001).

The onset of the Red Clay Sequence, which indicated enhanced aridity over the Asian continent, was also marked by a sudden increase in aeolian deposition in the North Pacific region (Zheng *et al.*, 2004). A more recent phase of the uplift of the Tibetan Plateau (ca. 3.6 Ma) effectively blocked Indian moisture sources from reaching East Asia and created conditions favorable for the development of the East Asian monsoon, which modulates the southward flow of cold, dry air masses across the East Asian continent in winter. As glacial cycles intensified, they enhanced conditions of stronger winds and higher aridity that favor dust emission during cold periods. Comparisons between loess and marine sediment records downwind of Asian deserts in the North Pacific Ocean suggest that dust deposition was enhanced by an order of magnitude following this later uplift event (Pettke *et al.*, 2000; Zheng *et al.*, 2004). The mineralogy and isotope chemistry of the deposited dust suggests that the source areas (basins north of the Tibetan Plateau as well as the Gobi desert) have remained basically the same since the onset of aridification, but have experienced different intensities of chemical weathering following the initiation of major Northern Hemisphere glacial cycles (Pettke *et al.*, 2000).

The onset of Northern Hemisphere glaciation has also affected the aridification and aeolian activity associated with Africa (DeMenocal, 2004). Marine sediment records of dust from both the North Atlantic and Arabian Sea also suggest a shift from a predominantly monsoon-driven climate toward more arid conditions after 2.8 Ma, modulated by the periodicity of Northern Hemisphere glaciations (DeMenocal, 1995). DeMenocal (2004) associates this increased aridity with the intensification of Northern Hemisphere glaciations, which resulted in cooler North Atlantic surface ocean temperatures that inhibited the expansion of the North African summer monsoon into the African continent, thereby increasing Saharan and Sahelian aridity.

4.13.3.2 The Distribution of Dust over the Last Glacial Period

Much information has been collected on dust deposition during the last glacial period. These data have been compiled using records from ice cores, marine sediments, and terrestrial records as part of the Dust Indicators and Records of Terrestrial and MArine Paleoenvironments (DIRTMAP) project (Kohfeld and Harrison, 2001), which was established to archive dust information for the last 130,000 years. The majority of this database is dedicated to the estimation of mass accumulation rates of dust for different time periods, for easy comparison with model simulations of the dust cycle (e.g., Mahowald *et al.*, 1999, 2006; Reader *et al.*, 2000; Tegen *et al.*, 2002; Werner *et al.*, 2003).

In addition to including some new marine sediment sites in the Equatorial Pacific Ocean (Anderson *et al.*, 2006) and new results from recent ice cores (Delmonte *et al.*, 2002, 2004a), the revised version of DIRTMAP provided here includes efforts to incorporate mass accumulation rates of last glacial loess deposits distributed around the world (Bettis *et al.*, 2003; Chlachula, 2003; Eden and Hammond, 2003; Frechen *et al.*, 2003; Hesse and McTainsh, 2003; Kohfeld and Harrison, 2003; Muhs *et al.*, 2003; Zárate, 2003). These data were recently published in a special issue of *Quaternary Science Reviews* (Derbyshire, 2003) and then compiled and included for a first time in comparison with model simulations of the last glacial period (Mahowald *et al.*, 2006). One difficulty in comparing loess accumulation rates with model simulations is that typical loess deposits show a particle size mode in the range 20–60 μm (Pye, 1987), which is larger than the grain sizes simulated by dust models of typically up to 10 μm. To facilitate a more realistic comparison with their particular model simulation, Mahowald *et al.* (2006) also estimated the fraction of loess sediments with grain size diameters smaller than 10 μm. However, here we present the bulk mass accumulation rates (Figures 3a and 3b).

The different records of glacial–interglacial changes in mineral dust deposition agree in showing increased dust fluxes during glacial periods. Ice core records, which are the longest distance from source regions, have demonstrated a 2–20-fold increase in deposition during the Last Glacial Maximum (LGM) compared to today (Figure 3c). Various patterns of deposition have been observed in marine sediments, but the overall change has been about two- to fivefold increase at the LGM. Land records have also demonstrated large changes in deposition rates over the last period of deglaciation. Highest rates of deposition during the last glacial period are recorded from Peoria Loess in the mid-continental United States, where deposition rates were as high as 17,500 $\mathrm{g\,m^{-2}\,yr^{-1}}$ during the last glacial period (Bettis *et al.*, 2003), and $\sim$3,500–11,500 $\mathrm{g\,m^{-2}\,yr^{-1}}$ on the deglaciation in central Nebraska (Roberts *et al.*, 2003). For comparison, the largest accumulation rates from the Chinese Loess Plateau were on the order of 1,000 $\mathrm{g\,m^{-2}\,yr^{-1}}$ (Sun *et al.*, 2000; Kohfeld and Harrison, 2003). Comprehensive estimates of changes in mass accumulation rates of dust have demonstrated approximately a threefold increase over the Chinese Loess Plateau between the last glacial period and late Holocene times (Sun *et al.*, 2000; Kohfeld and Harrison, 2003), a pattern that is repeated over multiple glacial–interglacial cycles (Sun and An, 2005).

The LGM has also been a major focus for dust modeling because both aeolian deposition rates and boundary conditions (e.g., insolation forcing, ice sheet extent, and atmospheric trace gas concentrations) are known with some confidence. Incorporating expanded dust source areas resulting from less extensive vegetation cover during glacial climate conditions increased the modeled atmospheric dust loads at high latitudes by factors of 1.4 up to 2.5, consistently with the high dust fluxes observed in polar ice cores (Mahowald *et al.*, 1999, 2006; Werner *et al.*, 2003). The potentially large effect of dust aerosol supplied by glacial outwash has been difficult to incorporate into global modeling schemes, largely because of the relatively small, subgrid-scale nature of glaciogenic processes. Using an inverse modeling scheme, Mahowald *et al.* (2006) infer that these glaciogenic sources increase glacial dust emissions by almost 60% over simulations that do not account for these sources. Still, potential increases in the extent of dry lake bed areas during the last glacial period, caused by the weakened hydrological cycle, have not yet been factored into global dust models, and these may also enhance dust emissions during glacial climates.

4.13.3.3 Glacial–Interglacial Cycles

The geologic record of mineral aerosols also demonstrates some intriguing temporal relationships between dust and atmospheric CO_2, as recorded in air bubbles of polar ice cores (Petit *et al.*, 1999). Close comparison between the dust concentration and atmospheric CO_2 concentrations in the Vostok ice core reveal that dust concentrations do not even begin to increase until atmospheric CO_2 values reach a critically low level of $\sim$220 ppm. In other words, atmospheric CO_2 levels seem to drop by $\sim$50 ppm below interglacial levels before dust concentrations even began to increase. Further examination of marine sediments demonstrates that this relationship may not be limited to the Vostok ice core, and may possibly be generalized to the entire ocean (Figure 4).

This relationship between CO_2 and dust is repeated over multiple glacial–interglacial cycles and is likely to represent an important recurring feedback between climate, CO_2, and dust. Model simulations of the last glacial period using the ECHAM3 climate model have demonstrated a significant increase in the areal extent of dust sources. This was a result of the response in plant evapotranspiration (and consequently vegetation cover) to changes in atmospheric CO_2 on glacial–interglacial timescales (Harrison and Prentice, 2003). Sensitivity studies suggested that about one-half of the increase in glacial dust emissions were thus due to the glacial reduction in atmospheric CO_2 (Mahowald *et al.*, 1999). The remaining changes in dust emissions were due to changes in vegetation cover in response to changed climate variables such as temperature and vegetation, as well as changes in wind speed and soil moisture that directly impact on dust emission fluxes. Recent simulations with the climate model CCM3 have included the effects of lower carbon dioxide on vegetation at the last glacial period, and resulted in a 35% increase in source areas. In simulations without the effects of lowered CO_2, including only the influence of glacial climate on vegetation, source area extent is only 15% greater than today (Mahowald *et al.*, 2006). These simulations suggest a mechanistic response between climate, atmospheric CO_2, and dust (see, e.g., Ridgwell and Watson, 2002).

4.13.4 MODERN RECORDS OF DUST

While geologic data provide some interesting insights into past changes in the dust cycle, a more extensive range of data describing different aspects of the modern dust cycle are available and can be used to constrain recent changes in the global dust cycle, and provide more detailed information about changes in dust emission, source area, transport, and deposition. For example, various *in situ* and remote-sensing applications allow quantification of several aspects of the atmospheric dust cycle.

4.13.4.1 Source Areas

Remote sensing with satellite instruments provides information on vegetation cover and surface properties that are a prerequisite for identification of dust source areas. Maps of surface conditions that are derived from satellites are used extensively in locating areas that are likely to act as preferential dust source areas, and these maps are frequently used as input parameters for modeling purposes (see Section 4.13.6). However, there are very few direct and spatially extensive measures of dust emissions.

Changes in visibility in response to atmospheric dust storms are qualitative indicators of changes in atmospheric dustiness close to source regions. A dust storm is defined as an event that reduces atmospheric visibility to $<$1 km due to the presence of dust. Several studies have used dust storm frequencies to describe wind erosion trends in specific regions (e.g., Changery, 1983; Middleton, 1984, 1986a, b; Wheaton and Chakravarti, 1990; Goudie and Middleton, 1992). Only one study (Engelstaedter *et al.*, 2003) has examined the global distribution of dust storms, using a climatological average of annual average dust storm frequency,

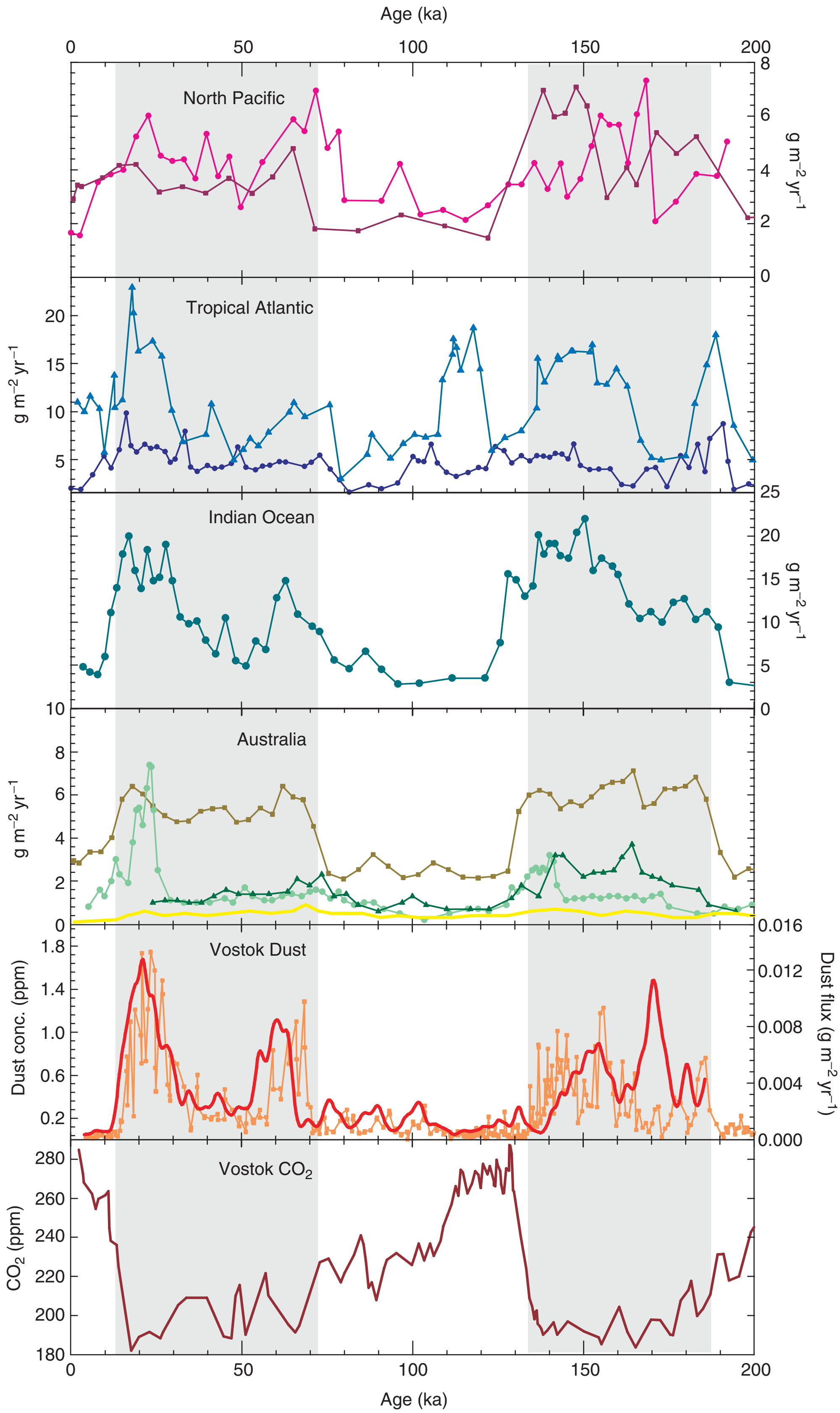
Age (ka)
North Pacific
g m^{-2} yr^{-1}
Tropical Atlantic
g m^{-2} yr^{-1}
Indian Ocean
g m^{-2} yr^{-1}
Australia
g m^{-2} yr^{-1}
Vostok Dust
Dust conc. (ppm)
Dust flux (g m^{-2} yr^{-1})
Vostok CO_2
CO_2 (ppm)
Age (ka)

approximately covering the time period 1970–1990 (Figure 5). That study demonstrated a statistical relationship between annual average dust storm frequency and land-surface conditions, in spite of the potential impact of atmospheric transport on visibility measurements. This relationship was also utilized later by Tegen *et al.* (2004a) to reassess the contribution of agricultural sources to the global dust emissions. However, this climatology does not allow for the examination of temporal changes in dust storm frequencies. Furthermore, in some cases the amount of data is too limited to produce statistically significant results, for example, for regional comparisons or when trying to establish relationships between dust storm frequency and degree of cultivation or soil protection (Tegen *et al.*, 2004a, b). Nevertheless, the currently available meteorological station data have the potential to provide a global time series of changes in dust storm frequencies that can be compared with model simulations over the past 50–100 years (Figure 5).

4.13.4.2 Transport

Modern satellite data retrievals provide a more direct means of measuring changes in dust transport than individual *in situ* measurements of dust concentration or deposition fluxes. However, quantification of dust optical thicknesses from such satellite retrievals requires *a priori* assumptions on dust optical properties, surface albedo, and the presence of cirrus clouds. *In situ* ground-based measurements offer the opportunity for long-term measurements that are difficult to achieve for satellite instruments.

Over the oceans, aerosol optical thickness products are derived from different satellite instrument retrievals, including Meteosat, AVHRR, SeaWifs, POLDER, MODIS, and MISR (for an overview see, e.g., Yu *et al.*, 2006). Generally, satellite measurements of light at specific wavelength that has been reflected by airborne particles and scattered back to space are used to quantify aerosol properties in cloud-free areas. This retrieval is impeded by light reflected from the Earth's surface, which can cause considerable uncertainties for aerosol retrievals above soils with high and variable surface reflectances. Over oceans with low surface albedo, aerosol optical thicknesses can be accurately retrieved from remote sensing. The estimate of dust optical thickness from these retrievals is complicated by the presence of other aerosols like sea-salt particles or anthropogenic sulfates and carbonaceous particles. Over land, qualitative distributions of aerosols absorbing at UV wavelengths are observed by the Total Ozone Mapping Spectrometer (TOMS) satellite (Hermann *et al.*, 1997) and more recently, Ozone Mapping Instruments (OMI, aboard the Aura satellite). Another instrument allowing for the retrieval of aerosols over some land surfaces is the Multiangle Imaging Spectro Radiometer (MISR) Instrument aboard the Terra satellite (Kahn *et al.*, 2005), which provides additional information by multiangular retrievals.

In addition to views from the air, the optical thickness of dust in the atmosphere can be estimated from the Earth's surface, using Sun photometers. The Aerosol Robotic Network (AERONET: Holben *et al.*, 1998) includes several hundred sites where sun and sky radiances are measured by intercalibrated sun photometers at four wavelengths (Figure 6). The retrieval algorithm inverts measurements of aerosol optical thickness and diffuse sky radiation and derives aerosol particle size distribution in the range from 0.05 to 15 μm and the complex refractive index at the four wavelengths (Dubovik and King, 2000). Several sites are located in or downwind of desert areas, and information from these sites can be used to determine the temporal variation of dust optical thickness and optical properties. AERONET retrievals are a useful ground validation tool for satellite retrievals and model estimates of aerosol optical thickness.

Although not a direct measure of transport, measurements of the atmospheric concentrations of dust, using mesh sampling and high-volume dust samplers, can provide an ongoing record of changes in dust concentrations over a

Figure 4 Changes in dust inputs to the ocean over the last 200,000 years as measured in marine sediment cores, as compared with dust deposition and changes in atmospheric CO_2 levels measured in the Vostok ice core. Shaded regions indicate time periods when atmospheric CO_2 concentrations dropped below 220 ppm, and coincide with periods of highest dust inputs to the Vostok ice core and each ocean basin. Terrigenous fluxes are from North Pacific cores H3571 (pink, 34.9° N, 179.7° E, 3571 m; Kawahata *et al.*, 2000) and S2612 (purple, 32.3° N, 157.8° E, 2612 m; Kawahata *et al.*, 1999); tropical Atlantic sites ODP 659 (light blue, 18.1° N, 21.0° W, 3082 m; Tiedemann *et al.*, 1994), and ODP 663 (blue, 1.2° S, 11.9° W, 3708 m; Schneider, 2002); Indian Ocean core RC27-61 (16.63° N, 59.86° E, 1806 m; Clemens and Prell, 1990), and Tasman Sea cores SO36-61 (yellow, 30.6° S, 161.4° E, 1340 m; Hesse, 1994), C1-86-6GC3 (green, 32.98° S, 160.0° E, 1540 m; Hesse, 1994), LH3166/NGC97 (35.5° S, 161.0° E, 3166 m; light green, Kawahata *et al.*, 1999, 2000), and E26.1 (brownish green, 40.3° S, 168.3° E, 910 m; Hesse, 1994). Adapted by permission of American Association for the Advancement of Science from Kohfeld *et al.* (2005).

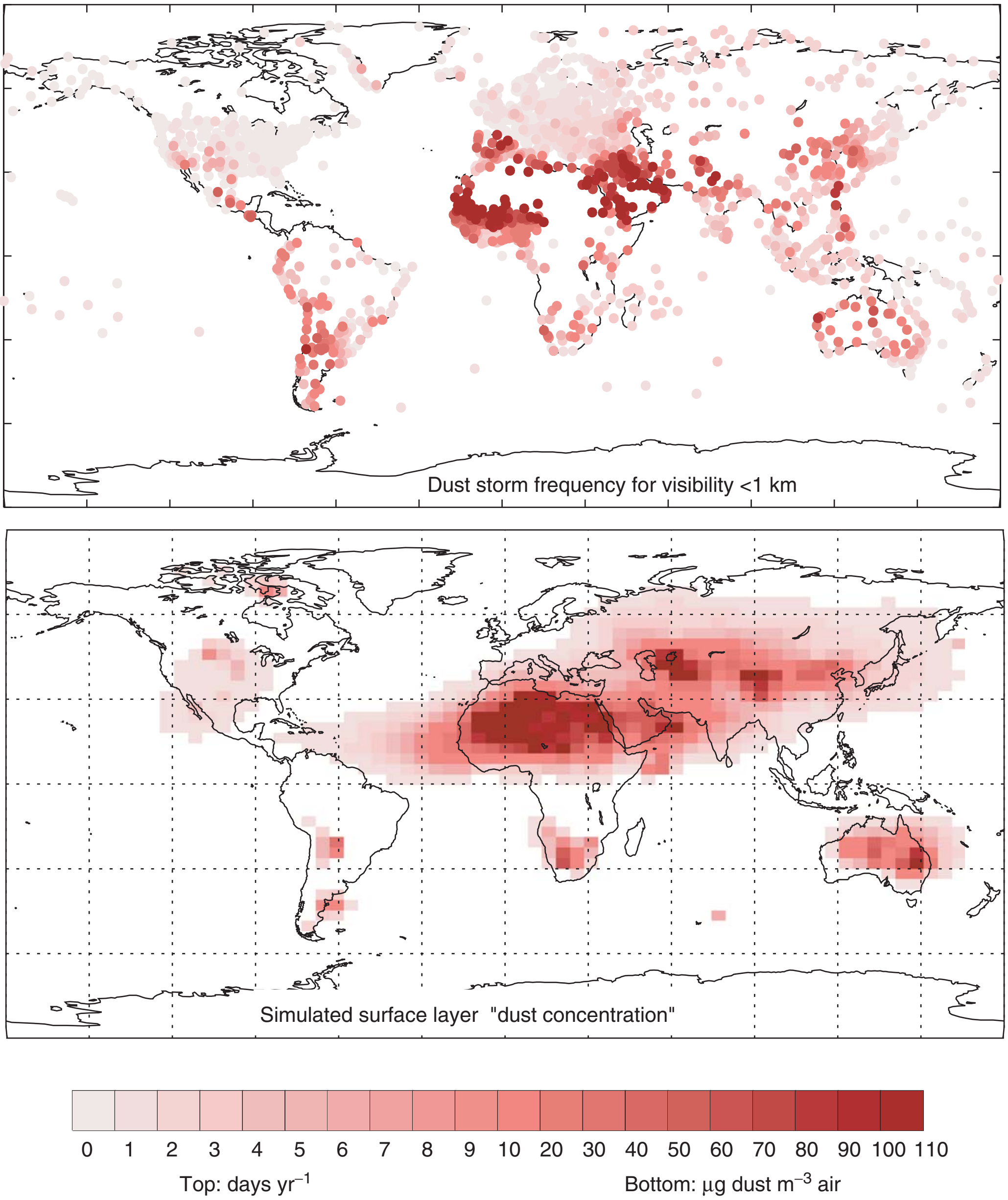

Figure 5 Climatology of annual dust storm frequency (days yr^{-1}) averaged from ~1971 to 1996 (Engelstaedter *et al.*, 2003) provides one semiquantitative means of approximating dust emissions. Here they are compared with output from a dust simulation of Tegen *et al.* (2002).

given site. Dust concentration information has been collected at several stations, as part of a network of mostly remote island sites (Prospero, 1996). These unique and very valuable long-term records have revealed such things as a long-term change in the transport of dust from Africa to the North American continent. Regional projects such as the Interagency Monitoring of Protected Visual Environments (IMPROVE) project in the United States have also attempted to measure changes in the atmospheric particulates. The IMPROVE project endeavores to quantify the soil dust contents of the atmosphere by measuring the total particle mass concentrations (as PM10 and PM2.5, which refers to particle mass of the particles with sizes of <10 and 2.5 µm, respectively). The program also approximates the total soil dust concentration from the trace metal composition of the collected samples. These analyses suggest that as much as 40% of the atmospheric particulates smaller than 2.5 µm in diameter in the southwestern United States are comprised of soil dust (Malm *et al.*, 2004).

In conclusion, *in situ* measurements allow quantification of dust properties, but have

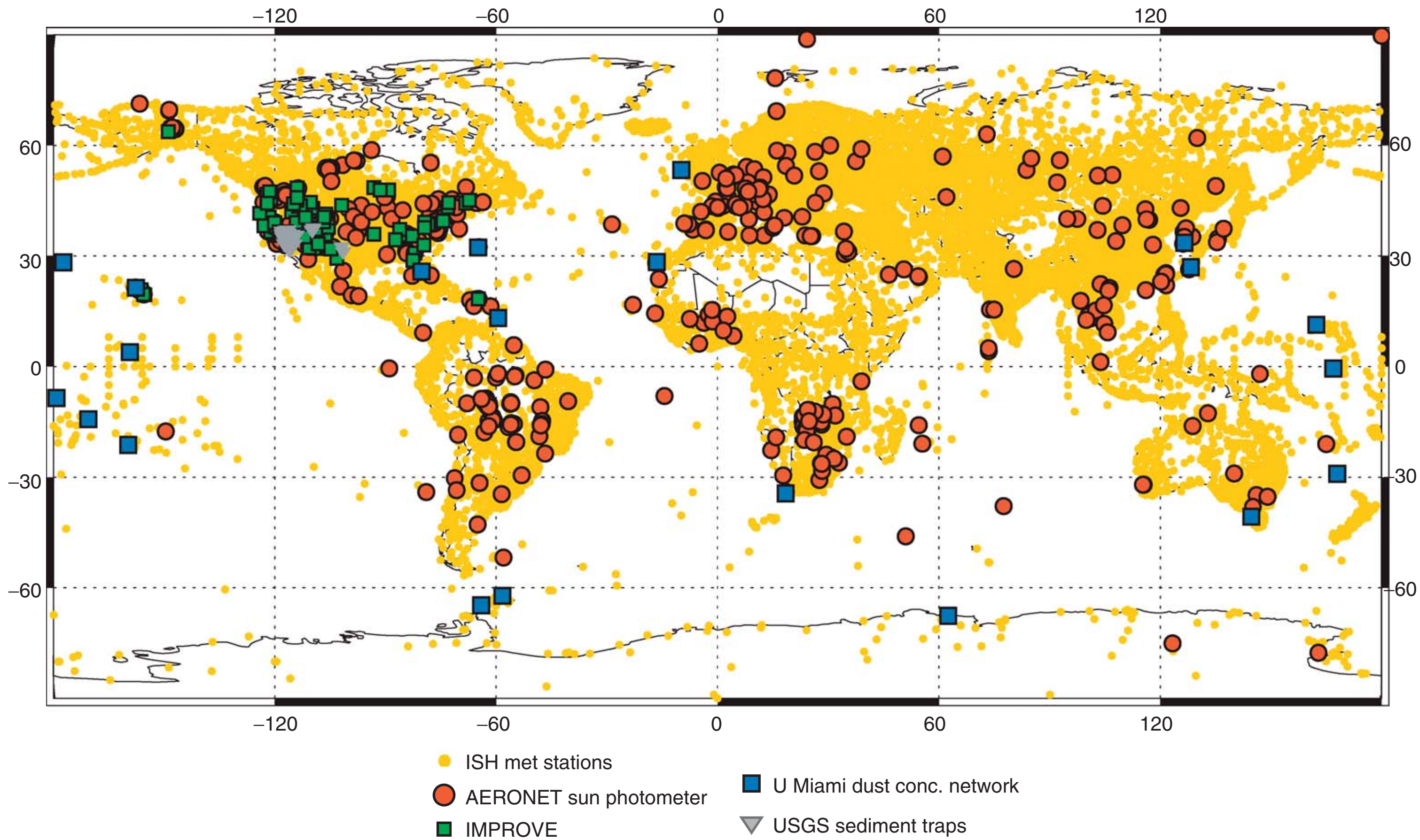

Figure 6 Summary of data available atmospheric optical thickness, visibility, dust particle concentration, and sediment deposition. These include the Integrated Surface Hourly meteorological station data available from the National Climatic Data Center (http://www4.ncdc.noaa.gov, June 2, 2006), AERONET sun photometer network (Holben *et al.*, 1998); Visibility, PM10, and PM2.5 measurements from IMPROVE stations started before 1995 (Malm *et al.*, 2004); a global network of atmospheric dust concentration measurements (Prospero, 1996); and data from dust sediment traps (Reheis, 2003).

usually only sparse spatial and temporal coverage. Reliable quantification of dust properties can only be achieved by combining several types of measurements and modeling (Figure 6).

4.13.4.3 Deposition

There are several means by which modern dust deposition can be measured, including land-based sediment traps (Reheis and Kihl, 1995), marine sediment traps (e.g., Honjo *et al.*, 2000), and snow samples in polar environments where dust falls directly on snow and ice (e.g., Bory *et al.*, 2002, 2003a, b). Few measurements determine both dry and wet deposition of dust particles simultaneously, which reduces the usefulness of such data (Mahowald *et al.*, 2005).

One difficulty of using land-based traps is the issue of calibrating the different trap architectures to demonstrate that quantitative estimates of dust fluxes are consistent. However, within a particular region using self-consistent traps, these traps have been able to provide examples of seasonal-to-interannual variability in dust deposition (e.g., Derbyshire *et al.*, 1998; Okin and Reheis, 2002). Thus, although difficult to interpret in the context of a global database, land-based traps have proved to be useful for understanding processes controlling regional dust cycle dynamics.

Marine-based sediment traps not only provide a means of measuring dust fluxes to the ocean surface, but also have complications. First, the terrigenous component must be isolated from the total flux of material using the same procedure as with marine sediments to remove the several biogenic minerals produced by organisms in the surface waters. As a result, sediment trap materials share the same uncertainties, especially at low fluxes. Furthermore, trace elements such as ^{232}Th show the same promise for reconstructing low dust fluxes (see Section 4.13.2.1).

A second issue is that dust that falls on the ocean surface must then be exported to the depth of the sediment trap. Phytoplankton and zooplankton activity can influence the aggregation process of dust particulates, and thus biogenic productivity can affect the seasonal timing of when these minerals are exported to the traps below (Bory and Newton, 2000; Bory *et al.*, 2001). Furthermore, minute dust particles can be horizontally advected or redistributed in the water column, before reaching the sediment trap. Several modeling (Siegel and Deuser, 1997) and observational (Gardner *et al.*, 1997) studies have attempted to quantify the extent of this problem, by taking into account particle sinking rates and horizontal velocities. The observational data from the Vema Channel suggested that while the horizontal fluxes past different traps varied by a factor of 37, the quantity collected by the traps deployed at various depths differed by only a factor of 1.4 (Gardner *et al.*, 1997). Alternatively, a modeling study suggested that for traps moored at water depths of 1,500 m, 95% of the collected materials fall within 600 km of the trap. Thirty percent of the material comes from within 200 km (Siegel and Armstrong, 2002). These distances lie in the order of magnitude of a single grid cell of a global transport model, which usually has a length of 200–500 km in one dimension. Thus, as with all data, it is important to be aware of the potential limitations when interpreting these dust flux data.

A third means of measuring dust deposition is through quantification of the particulates that land on ice and snow, both in polar and alpine regions. Quantification of deposition from these regimes requires a precise estimation of snow accumulation rates. Furthermore, chemical analyses on mineral dust can be complicated in regions that experience seasonal melt layers. Nevertheless, snow pit studies in locations such as Greenland have collected sufficient quantities of snow to isolate seasonal changes in Asian dust sources to the ice sheet (Bory *et al.*, 2002, 2003a, b).

4.13.5 MODERN VARIABILITY OF THE DUST CYCLE

Quantifying changes in modern variability of dust emissions and transport requires detailed datasets appropriate for addressing the changes we wish to study. The previous section reviewed several types of data for assessing the inter- and intra-annual variability of atmospheric dust. Currently, there exists no global dataset that allows both a data and modeling analysis of systematic changes in dust emissions over the past several decades.

Nevertheless, enough data have been collected to document changes in the processes associated with the dust cycle that have varied over the last 100 years. Changes in dust emissions can be modified by anthropogenic influences either directly by land use, or indirectly through changes in surface wind speed, the hydrological cycle, or vegetation changes as a consequence of anthropogenic climate changes (Zender *et al.*, 2004). Model results suggest that the emissions and atmospheric dust loading since preindustrial times may have altered considerably due to changes in climate and vegetation cover (Mahowald and Luo, 2003) The authors of this study conclude that the dust loads may have increased by up to 24% or decreased up to 60% for different climate and land-use scenarios. The uncertain and sparse observations available for validating those results make it difficult to decide which of the scenarios is the most probable.

Some regions have experienced dramatic changes in dust production, such as in the North American dust bowl region (e.g., Goudie and Middleton, 1992), the Sahel region of West Africa (Mbourou *et al.*, 1997; Prospero and Lamb, 2003), and Australia (McTainsh *et al.*, 1998). Recent dust storm frequency analyses in China have also shown that the 1950s–1960s were much dustier than today (Zhao *et al.*, 2004). Thus, the modern records provide vidence of interdecadal variability in dust production.

During the past decades, there have been several documented changes in regional land surface conditions such as vegetation cover, and trends in temperature and precipitation that are superimposed on observed climate fluctuations such as the El Niño/Southern Oscillation and the North Atlantic Oscillation (Houghton *et al.*, 2001), which can be related to changes in the atmospheric dust content. For example, Okin and Reheis (2002) use dust flux data to support a correlation between dust events in the southwestern United States and the previous year's winter temperature anomalies from the Equatorial Pacific Ocean. They suggest that reduced precipitation during La Niña years results in less vegetation cover and enhanced dust activity in the southwestern United States. However, their results also suggest that enhanced precipitation and flooding associated with the strongest El Niño years results in a renewal of reworked material to closed basins, making it subsequently available for transport.

Multiyear dust aerosol retrievals from the Meteosat satellite indicate a correlation of dust transport toward the Mediterranean and the North Atlantic with the North Atlantic Oscillation (NAO) (Moulin *et al.*, 1997). Recent model simulations also suggest that interannual variability in winter dust production in the Sahel desert region is likely correlated to changes in the NAO, but such variability is not apparent in dust concentration records in Barbados which integrate both emission and transport changes (Ginoux *et al.*, 2004). Testing the significance of these correlations is problematic due to the decadal-scale variability of the NAO and short timescale of most dust records. In contrast, Moulin and Chiapello (2004) and Chiapello *et al.* (2005) find observational evidence of a connection between multiyear satellite retrievals from the TOMS and Meteosat instruments, the dust concentration record at Barbados, and the Sahel drought. Analysis of the potential connections between these factors requires an integrated approach combining the different observations and model results.

4.13.6 FILLING IN THE GAPS: THE ROLE OF GLOBAL DUST CYCLE MODELS

Most measurements of dust properties provide only patchy and discrete information (both in time and space). This patchiness complicates any global assessment of the spatial and temporal variability in the emissions, the atmospheric burden, transport, and deposition of dust. Global dust models allow us to fill in the gaps. When validated against the existing data, global models allow us to assess changes in source areas. They can account for the integrated impact of wind speeds, transport, and deposition processes on large-scale spatial deposition patterns. Finally, global dust models can provide a first-order estimate on changes in dust emissions and the atmospheric burden of dust for geologic, modern, and future time periods.

To better understand processes that control dust emission and deposition, quantify atmospheric loads, and estimate dust effects, not only for present-day but also for past climates or projections of future changes, increasingly complex regional and global-scale models of the dust cycle have been developed in the recent years (Zender *et al.*, 2004). Dust emissions in such models are determined by surface wind speeds, and surface properties such as roughness length, vegetation cover, soil moisture, and soil texture. Recently, developed dust models explicitly prescribe seasonal vegetation cover to delimit the extent of dust sources (Werner *et al.*, 2003) as well as use topographic depressions in dry, unvegetated areas as indicators of preferential sources containing fine and loose sediment particles that can be easily deflated under strong wind conditions (Ginoux *et al.*, 2001). Surface roughness retrievals from the POLarization and Directionality of the Earth's Reflectances (POLDER) instrument (Laurent *et al.*, 2005) or the European Remote Sensing (ERS) microwave scatterometer (Prigent *et al.*, 2005) are used as input parameters in large-scale dust emission models, substantially improving distribution and magnitudes of calculated dust emission fluxes compared with the assumption of a constant surface roughness in the emission model. Other large-scale datasets of soil properties like texture are difficult to obtain, as the most active dust sources lie in remote areas that cannot easily be accessed.

Global models are able to simulate the distribution of atmospheric dust, the seasonal and interannual changes, and the magnitude of optical thickness reasonably well. Major remaining problems in computing global dust emissions from wind deflation include the unavailability of soil properties datasets at global scale, and insufficient model resolution, as peak gusts that are responsible for the strongest dust events remain largely unresolved in large-scale global models. Parameterizations of subgrid-scale variability in surface winds (e.g., Cakmur *et al.*, 2004; Grini *et al.*, 2005) have provided some improvements in computations of dust emissions. Regional models of dust emission, transport, and deposition resolve surface wind speed variability better than global models, and are well suited for investigations of individual dust events and comparisons with *in situ* observations made during field experiments. Regional dust models exist for key regions, including the Sahara and Asia (Sokolik *et al.*, 2001). However, while the topography, soil conditions, and small-scale extreme wind events are simulated more realistically in regional compared to global models, uncertainties in the parameterization of key processes and input data on meteorological fields and soil properties still remain.

Projections of dust emissions taking into account expected changes in vegetation and meteorology in the next 100 years yield changes ranging from a 60% decrease (Mahowald *et al.*, 2006) to a 233% increase in dust (Woodward *et al.*, 2005). The large difference in those studies is mostly related to the difference in predicted expansion or shrinking of the desert regions, from which dust aerosol can be emitted, by the different vegetation models used in the studies. Mahowald *et al.* (2006) used an equilibrium-vegetation model and predicted a maximum reduction in dust emissions, including a substantial reduction of the size of the Saharan desert. Alternatively, Woodward *et al.* (2005) used a dynamic, coupled vegetation–climate model and predicted maximum increase in dust emission, largely as a result of desertification of the Amazon rainforest region.

Agricultural land use and other human disturbances such as off-road traffic construction can increase soil dust emission. The degree to which anthropogenically disturbed soils add to the regional and global dust loading is still unclear. Comparison of model estimates with available observations from remote-sensing and meteorological data lead to estimates that disturbed soils contribute between $<10\%$ and up to 50% of the modern global dust load in the atmosphere (Houghton *et al.*, 2001; Tegen *et al.*, 2004a, b; Mahowald *et al.*, 2004). The ability of current dust cycle models to assess these changes represents progress in the field. At the same time, the uncertainty in the modeled responses demonstrates the future challenges for assessing the role of dust that lies ahead.

4.13.7 DUST FEEDBACKS WITHIN THE EARTH SYSTEM

4.13.7.1 Radiative Feedbacks

A major climate impact of dust aerosols is its direct radiative forcing (Houghton *et al.*, 2001). Dust particles reflect part of the incoming solar radiation back to space, thus reducing the radiative fluxes reaching the surface. The sign and magnitude of the impact of dust particles on solar radiation depends on dust optical properties, the albedo of the underlying surface and cloud cover (e.g., Liao and Seinfeld, 1998). Beneath dust clouds this effect can locally reduce the direct solar fluxes more than $100\,\mathrm{W\,m^{-2}}$ (e.g., Haywood *et al.*, 2003a, b). For reference, the mean annual incident solar radiation is $\sim 342\,\mathrm{W\,m^{-2}}$ at the top of the atmosphere. Incoming sunlight can also be absorbed by dust particles, which can heat the dust layer and result in a redistribution of energy within the atmospheric column. The relation between absorbed and reflected solar radiation depends on the size and mineral composition of the dust particles (Sokolik *et al.*, 2001). Recent *in situ* retrievals of dust optical properties from sun photometer measurements suggest dust only to be weakly absorbing at solar wavelengths (Dubovik *et al.*, 2002). Owing to their large sizes, dust particles also contribute to the greenhouse effect by absorbing and emitting outgoing terrestrial radiation. This effect depends on the vertical distribution of dust, and is expected to be smaller than the solar effect (Houghton *et al.*, 2001).

Haywood *et al.* (2005) recently estimated a longwave radiative effect of up to $+50\,\mathrm{W\,m^{-2}}$ in cloud-free regions of the Sahara. Based on our current knowledge of the optical properties and distribution of dust aerosol, its net radiative effect is expected to be negative in the global mean, such that an increase of atmospheric dust load leads to a reduction of energy input into the earth system. This causes not only reduced surface temperatures in the presence of dust clouds, but also a weakening of the hydrological cycle due to reduced evaporation beneath dust clouds (Miller *et al.*, 2004). The direct radiative forcing by dust aerosol leads to a stabilizing of the dust-laden atmosphere and to a feedback on the dust production itself;

reduced surface winds reduce dust emissions in a global model by 10–20% if the dust radiative effect is taken into consideration (Perlwitz *et al.*, 2001). While a positive feedback of dust forcing upon dust production and atmospheric dust load is imaginable due to reduced precipitation enhancing the availability of dust particles for deflation and reduced wet removal from the atmosphere, model results by, for example, Perlwitz *et al.* (2001) indicate that the negative-feedback processes are dominant.

Both the regional and global radiative impacts of dust would be expected to change under different climate conditions when the overall distribution and total atmospheric burden of dust are expected to be different. Early studies hypothesized that atmospheric dust over ice sheets with high-surface albedos in high-latitude regions could create localized heating (Peltier and Marshall, 1995). Global model simulations suggested that dust over ice sheets could result in a surface warming of as much as 1–4 °C over Greenland and North America (Overpeck *et al.*, 1996). The authors suggested that this heating could be sufficient to invoke rapid melting at the edges of ice sheets and provide a sufficient feedback to cause rapid climate events that were propagated through the climate system. Later, investigations using more realistic simulations of dust suggested that the largest radiative impacts of dust were found in the tropical regions, with an overall negative top-of-atmosphere (TOA) forcing of $\sim$2–3 $\mathrm{W\,m^{-2}}$ associated with the largest dust sources (Claquin *et al.*, 2003). This forcing was of the same order of magnitude as the radiative cooling effect associated with the glacial reduction in atmospheric carbon dioxide.

In high latitudes, the TOA radiative forcing was dominated by the negative forcing of nearly $-20\,\mathrm{W\,m^{-2}}$ associated with albedo effects from greatly expanded Northern Hemisphere ice sheets (Claquin *et al.*, 2003). Only a slightly positive forcing due to dust was found over high-latitude ice sheets, as atmospheric dust loadings were very low (even though greatly enhanced compared to interglacial time periods). One interesting point about these simulations is that global model experiments have not been able to sufficiently capture the changes in dust associated with glacial conditions. Simulated dust accumulation rates have been underestimated in China (Kohfeld and Harrison, 2003) and in particular in the mid-continental United States, where the highest mass accumulation rates of dust have been recorded (Roberts *et al.*, 2003) on the deglaciation. Roberts *et al.* (2003) suggested that the atmospheric dust may be a missing feedback that is needed to account for the difference between the simulated late glacial warming in this region (e.g., Bartlein *et al.*, 1998) and the observed vegetation and fauna that indicate that the region remained cool well into the deglaciation. Recent model simulations have used an optimization approach to infer the potential contributions of glaciogenic sources to atmospheric dust loadings at the LGM (Mahowald *et al.*, 2006). The inclusion of these glaciogenic sources results in a regional enhancement of the TOA radiative forcing by 1–5 $\mathrm{W\,m^{-2}}$ at the ice sheet edge in North America (Mahowald *et al.*, in press), but also a localized cooling of the same magnitude just to the south of the ice sheet in the region of these high dust accumulation rates. This suggests that indeed regional radiative impacts of dust may be large enough to impact the energy balance of climate and ice sheet ablation.

Very few estimates have been made of future changes in the radiative forcing of dust. The results of future changes in globally averaged radiative forcing by dust estimated in the independent studies by Woodward *et al.* (2005) and Mahowald *et al.* (in press) are actually quite close with an increase by $+0.17$ and $+0.14\,\mathrm{W\,m^{-2}}$, respectively, but these results are obtained for entirely different reasons. Woodward *et al.* estimated a fivefold increase in TOA forcing by dust between 2000 and 2100, increasing from 0.04 to 0.21 $\mathrm{W\,m^{-2}}$. This increase in forcing is a consequence of increased dust emissions and an originally positive dust forcing. Alternatively, Mahowald *et al.* (in press) estimated a less-negative TOA dust forcing for future climate conditions as a consequence of reduced dust emissions with a negative dust forcing estimate for modern climate conditions. In each instance, the globally averaged impacts of dust are small. However, regional impacts could be substantial (e.g., $>10\,\mathrm{W\,m^{-2}}$ change in dust forcing in the Amazon basin in the Woodward *et al.* (2005) estimate). Furthermore, the potential for indirect effects of dust on cloud formation and precipitation may prove more significant. In particular, the role of dust aerosol particles in providing nuclei for ice cloud formation may be important (DeMott *et al.*, 2003). This is an area that requires much future work because the variability between different climate model simulations is larger than the changes in future dustiness themselves, and the indirect aerosol effects require further investigation.

4.13.7.2 Biogeochemical Feedbacks

Dust has also been recognized as a potential source of nutrients to both terrestrial and marine ecosystems. Several studies have documented the aeolian input of dust to soils (Chadwick and Davis, 1990; Muhs *et al.*, 1990; Tiessen *et al.*, 1991; Swap *et al.*, 1992; Chadwick *et al.*, 1999; Vitousek *et al.*, 1999; Reynolds *et al.*, 2006). In regions such as Hawaii where soils are formed on fresh basalts, near-surface layers contain as much as 30% aeolian-derived quartz (Kurtz *et al.*, 2001). Saharan dust has been suggested as a source of potassium and calcium to topsoils in Ghana (Tiessen *et al.*, 1991) as well as a long-term source of trace elements to the Amazon basin (Swap *et al.*, 1992). Recent work on the Colorado Plateau suggests that aeolian inputs provide as much as 40–80% of plant nutrients (Reynolds *et al.*, 2006). One implication is that changes in dust emissions, transport, and deposition can affect terrestrial ecosystems on geologic timescales but also on modern ones. For example, Reheis *et al.* (2002) demonstrate that certain geochemical "hot spots," such as Owens Valley, California, have the potential to contribute toxic metals to soils in the southwestern United States, and that the impacts of these contributions are still relatively unstudied.

Dust is also an important external source of nutrients, particularly iron, to the ocean (Duce *et al.*, 1991; Prospero, 1996; Jickells *et al.*, 2005). Atmospheric dust has a relatively low iron content (3.5%), and it is estimated that on average <2% of that iron is soluble in seawater. However, because most of the fluvial and glacially derived iron is trapped in coastal regions, aeolian dust becomes a necessary source of iron to relieve this limitation (for review see Jickells *et al.*, 2005). Several laboratory (e.g., Martin and Fitzwater, 1988) and *in situ* experiments (for summary see de Baar *et al.*, 2005) have demonstrated the potential of Fe for enhancing phytoplankton productivity and carbon uptake in Fe-limited regions. Furthermore, observations of natural dust-fertilization events (Bishop *et al.*, 2002) have shown that Asian dust is a significant source of iron to Pacific Ocean waters today, and the sediment record shows significant fluctuations in dust influxes on glacial–interglacial timescales. A long-standing hypothesis (Martin, 1990) holds that increased iron supply during glacial times invigorated the ocean's biological pump, and thus drew down atmospheric CO_2. Studies invoking Fe-enhancement of the biological pump focused on the Southern Ocean because of the large inventory of unused surface nutrients and the strong connection between surface and CO_2-rich deep waters. Several modeling and data studies have examined the response of marine biota to iron fertilization from dust and suggested that this effect could account for between a 10 and 40 ppm reduction in atmospheric CO_2 levels during the last glacial period (Archer *et al.*, 2000; Watson *et al.*, 2000; Bopp *et al.*, 2003; Kohfeld *et al.*, 2005). In other words, the iron fertilization effects of dust could account for a substantial portion of the glacial–interglacial changes in atmospheric CO_2, but it is not likely to explain the entire 80–100 ppm change observed in ice core records.

4.13.8 FUTURE OUTLOOK

Biogeochemical modeling studies have focused mostly on the impact of iron fertilization in the modern and glacial oceans, with little emphasis to date on the potential biogeochemical impacts of future changes in dust emissions due to climate and anthropogenic activity (Ridgwell and Kohfeld, in press). To date, the projected changes in dust emissions by 2100 range from decreases of 60% (Mahowald *et al.*, 2006) to increases of 233% (Woodward *et al.*, 2005) in response to climate changes. An increase in dust emissions by 233%, while extreme, is of the same order of the glacial–interglacial changes in dust inputs to the ocean, and thus the projected biogeochemical impacts could be quite substantial. While the radiative impacts of these changes have been studied, the biogeochemical feedbacks are only beginning to be considered in projections of future climate change (e.g., Ridgwell *et al.*, 2002; Parekh *et al.*, 2006). Yet, how can we improve our understanding of the dust cycle to understand even the sign of change in the future atmospheric dust burden?

Sophisticated models of the dust cycle are now able to reproduce the characteristics of global and regional dust distribution for modern and glacial climates, the diverging results in different future estimates of atmospheric dust show, however, that the connection between dust emissions and climate are not yet sufficiently understood. The role of vegetation changes and thus the changes in the extent of dust sources remains a major uncertainty factor in dust–climate models.

One means of improving our understanding of the relationship between dust emissions, climate, and human activity is to expand our data coverage in the time domain. For example, utilizing the full extent of global meteorological station data (including visibility, humidity, precipitation, wind speed, and gustiness) may allow us to quantify changes in global dust storm frequencies over the past century. Alternatively, in the past 10 years, vast improvements have been made in global syntheses of geologic data of dust deposition, but more work could be done. For example, sedimentary records of dust can be normalized using constant flux proxies to help account for problems of sediment redistribution.

Use of geochemical sediment tracers such as ^{232}Th (e.g., Chase *et al.*, 2001; Anderson *et al.*, 2006) can also help eliminate the methodological uncertainties associated with isolating terrigenous materials from the dominant biogenic materials found in sediment cores, thus making reconstructions of changes in dust fluxes to the ocean more reliable. Finally, an important goal of these datasets is to make them comparable to modeled output of the dust cycle. The DIRTMAP database (Kohfeld and Harrison, 2001) was one step in this direction in that data from multiple paleoenvironments were interpreted in terms of their mass fluxes so that they could be compared with modeled output. Another step in this direction has been made by estimating the portion of terrestrial loess deposits that can be directly compared with model simulations, for example, by isolating the grain sizes that are actually transported by certain modeling schemes (Mahowald *et al.*, 2006). This effort has been one step in the direction of understanding the role of near-source loess deposits in the global dust cycle (and its resultant impact on climate).

Another avenue for advancement in our ability to simulate changes in dust sources and emissions lies in expanding our current observational networks for measuring changes in dust emissions and transport. New observations of dust distribution and properties from upcoming satellite missions (as e.g., the lidar measurements of vertical distribution of aerosol and cloud properties with the Cloud-Aerosol Lidar and Infrared Pathfinder Satellite Observations (CALIPSO) instrument and field experiments (such as AMMA: African Monsoon Multidisciplinary Analysis and SAMUM: SAharan Mineral dUst ExperiMent, in the southern and northern Sahara, respectively, with field measurements during 2006) will greatly enhance our knowledge on dust properties and dust production and transport. Global proxies of dust emissions also hold great promise, as does increasing efforts to use multiple datasets to constrain model simulations (e.g., Cakmur *et al.*, 2006).

ACKNOWLEDGMENTS

We thank D. Muhs and N. Mahowald for graciously providing the global compilation of terrestrial loess mass accumulation rates and other unpublished data for the improvement of this work.

REFERENCES

Aleinikoff J. N., Muhs D., Sauer R. R., and Fanning C. M. (1999) Late Quaternary loess in northeastern Colorado. Part II: Pb isotopic evidence for the variability of loess sources. *Geol. Soc. Am. Bull.* **111**, 1876–1883.

Alfaro S. C., Gaudichet A., Gomes L., and Maille M. (1998) Mineral aerosol production by wind erosion: aerosol particle sizes and binding energies. *Geophys. Res. Lett.* **25**, 991–994.

Alley R. B., Finkel R. C., Nishizumi K., Anankakrishnan S., Shuman C. A., Mershon G., Zielinski G. A., and Mayewski P. A. (1995) Changes in continental and sea-salt atmospheric loadings in central Greenland during the most recent deglaciation: model-based estimates. *J. Glaciol.* **41**, 503–514.

An Z. S. (2000) The history and variability of East Asian Paleomonsoon climate. *Quat. Sci. Rev.* **19**, 171–187.

Anderson R. F., Fleisher M. Q., and Lao Y. (2006) Glacial–interglacial variability in the delivery of dust to the central equatorial Pacific Ocean. *Earth Planet. Sci. Lett.* **242**, 406–414.

Archer D., Winguth A., Lea D., and Mahowald N. (2000) What caused the glacial/interglacial atmospheric pCO_2 cycles? *Rev. Geophys.* **38**, 159–189.

Bartlein P. J., Anderson K. H., Anderson P. M., Edwards M. E., Mock C. J., Thompson R. S., Webb R. S., Webb T., III, and Whitlock C. (1998) Paleoclimate simulations for North America over the past 21,000 years: features of the simulated climate and comparisons with paleoenvironmental data. *Quat. Sci. Rev.* **17**, 549–586.

Basile I., Grousset F. E., Revel M., Petit J. R., Biscaye P. E., and Barkov N. I. (1997) Patagonian origin of glacial dust deposited in East Antarctica (Vostok and Dome C) during glacial stages 2, 4 and 6. *Earth Planet. Sci. Lett.* **146**, 573–589.

Bettis E. A., III, Muhs D. R., Roberts H. M., and Wintle A. G. (2003) Last Glacial loess in the conterminous USA. *Quat. Sci. Rev.* **22**, 1907–1946.

Biscaye P. E. (1965) Mineralogy and sedimentation of recent deep-sea clay in the Atlantic Ocean and adjacent seas and oceans. *Geol. Soc. Am. Bull.* **76**, 732–803.

Biscaye P. E., Grousset F. E., Revel M., Van der Gaast S., Zielinski G. A., Vaars A., and Kukla G. (1997) Asian provenance of glacial dust (Stage 2) in the GISP2 ice core, Summit, Greenland. *J. Geophys. Res.* **102**, 26315–26886.

Bishop J. K. B., Davis R. E., and Sherman J. T. (2002) Robotic observations of dust storm enhancement of carbon biomass in the North Pacific. *Science* **298**, 817–821.

Bopp L., Kohfeld K. E., Le Quéré C., and Aumont O. (2003) Dust impact on marine biota and atmospheric CO_2 during glacial periods. *Paleoceanography* **18**, doi:10.1029/2002PA000810.

Bory A. J.-M., Biscaye P. E., and Grousset P. E. (2003a) Two distinct seasonal Asian source regions for mineral dust deposited in Greenland (NorthGRIP). *Geophys. Res. Lett.* **30**, 1167.

Bory A. J.-M., Biscaye P. E., Piotrowski A. M., and Steffensen J. P. (2003b) Regional variability of ice core dust composition and provenance in Greenland. *Geochem., Geophys., Geosyst.* **4**, 1107.

Bory A. J.-M., Biscaye P. E., Svensson A., and Grousset F. E. (2002) Seasonal variability in the origin of recent atmospheric mineral dust at NorthGRIP, Greenland. *Earth Planet. Sci. Lett.* **196**, 123–134.

Bory A., Jeandel C., Leblond N., Vangriesheim A., Khripounoff A., Beaufort L., Rabouille C., Nicolas E., Tachikawa K., Etcheber H., and Buat-Ménard P. (2001) Downward particle fluxes within different productivity regimes off the Mauritanian upwelling zone (EUMELI program). *Deep-Sea Res. I* **48**, 2251–2282.

Bory A. J.-M. and Newton P. P. (2000) Transport of airborne lithogenic material down through the water column in two contrasting regions of the eastern subtropical North Atlantic Ocean. *Global Biogeochem. Cycles* **14**, 297–315.

Briat M., Royer A., Petit J. R., and Lorius C. (1982) Late glacial input of eolian continental dust in the Dome C ice core: additional evidence from individual microparticle analysis. *Ann. Glaciaol.* **3**, 27–30.

Cakmur R., Miller R., Perlwitz J., Geogdzhayev I., Ginoux P., Koch D., Kohfeld K., Tegen I., and Zender C. (2006) Constraining the global dust emission and load by minimizing the difference between the model and observations. *J. Geophys. Res.—Atmos.* **111**, Art. No. D06207.

Cakmur R., Miller R., and Torres O. (2004) Incorporating the effect of small-scale circulations upon dust emission in an atmospheric general circulation model. *J. Geophys. Res.—Atmos.* **109**, Art. No. D07201.

Cannon W. F., Dean W. E., and Bullock J. H., Jr. (2003) Effects of Holocene climate change on mercury deposition in Elk Lake, Minnesota: the importance of eolian transport in the mercury cycle. *Geology* **31**, 187–190.

Chadwick A. O. and Davis J. O. (1990) Soil-forming intervals causeed by eolian sediment pulses in the Lahontan Basin, northwestern Nevada. *Geology* **18**, 243–246.

Chadwick O. A., Derry L. A., Vitousek P. M., Huebert B. J., and Hedin L. O. (1999) Changing sources of nutrients during four million years of ecosystem development. *Nature* **397**, 491–497.

Changery M. J. (1983) *A Dust Climatology of the Western United States*. NUREG/CR-3211. US Nuclear Requlatory Commission, Washington, DC, Contract No. NRC-01-78-015, 42pp.

Chase Z., Anderson R. F., and Fleisher M. Q. (2001) Evidence from authigenic uranium for increased productivity of the glacial Subantarctic Ocean. *Paleoceanography* **16**, 468–478.

Chiapello I., Moulin C., and Prospero J. (2005) Understanding the long-term variability of African dust transport across the Atlantic as recorded in both Barbados surface concentrations and large-scale Total Ozone Mapping Spectrometer (TOMS) optical thickness. *J. Geophys. Res.—Atmos.* **110**, Art. No. D18S10.

Chlachula J. (2003) The Siberian loess record and its significance for reconstruction of Pleistocene climate change in north-central Asia. *Quat. Sci. Rev.* **22**, 1879–1906.

Claquin T., Roelandt C., Kohfeld K. E., Harrison S. P., Tegen I., Prentice I. C., Balkanski Y., Bergametti G., Hansson M., Mahowald N., Rodhe H., and Schulz M. (2003) Radiative forcing of climate by ice-age atmospheric dust. *Clim. Dynam.* **20**, 193–202, doi:10.1007/s00382-002-0269-1.

Claquin T., Schulz M., and Balkanski Y. (1999) Modeling the mineralogy of atmospheric dust sources. *J. Geophys. Res.* **104**, 22243–22256.

Clemens S. C. (1998) Dust response to seasonal atmospheric forcing: proxy evaluation and calibration. *Paleoceanography* **13**, 471–490.

Clemens S. C. and Prell W. L. (1990) Late Pleistocene variability of Arabian Sea summer monsoon winds and continental aridity: eolian records from the lithogenic component of deep-sea sediments. *Paleoceanography* **5**, 109–145.

De Angelis M., Legrand M., Petit J. R., Barkov N. I., Korotkevitch Y. S., and Kotlyakov V. M. (1984) Soluble and insoluble impurities along the 950 m deep Vostok ice core (Antarctica)—climate implications. *J. Atmos. Chem.* **1**, 215–239.

de Baar H. J. W., Boyd P. W., Coale K. H., Landry M. R., Tsuda A., Assmy P., Bakker D. C. E., Bozec Y., Barber R., Brzezinski M. A., Buesseler K. O., Boye′ M., Croot P. L., Gervais F., Gorbunov M. Y., Harrison P. J., Hiscock M. R., Laan P., Lancelot C., Law C. S., Levasseur M., Marchetti A., Millero F. J., Nishioka J., Nojiri Y., van Oijen T., Riebesell U., Rijkenberg M. J. A., Saito H., Takeda S., Timmermans K. R., Veldhuis M. J. W., Waite A. M., and Wong C.-S. (2005) Synthesis of iron fertilization experiments: from the Iron Age in the Age of Enlightenment. *J. Geophys. Res.* **110**, doi:10.1029/2004JC002601.

Delmonte B., Basile-Doelsch I., Petit J. R., Maggi V., Revel-Rolland M., Michard A., Jagoutz E., and Grousset F. (2004a) Comparing the Epica and Vostok dust records during the last 220,000 years: stratigraphical correlation and provenance in glacial periods. *Earth Sci. Rev.* **66**, 63–87.

Delmonte B., Petit J. R., Basile-Doelsch I., Maggi V., and Ya Lipenkov V. (2004b) Dust size evidence for opposite regional atmospheric circulation changes over east Antarctica during the last climatic transition. *Clim. Dynam.* **23**, 427–438.

Delmonte B., Petit J. R., and Maggi V. (2002) Glacial to Holocene implications of the new 27000-year dust record from the EPICA Dome C (East Antarctica) ice core. *Clim. Dynam.* **18**, 647–660.

deMenocal P. B. (1995) Plio-Pleistocene African climate. *Science* **270**, 53–59.

deMenocal P. B. (2004) African climate change and faunal evolution during the Pliocene–Pleistocene. *Earth Planet. Sci. Lett.* **220**, 2–24.

DeMott P. J., Sassen K., Poellot M. R., Baumgardner D., Rogers D. C., Brooks S. D., Prenni A. J., and Kreidenweis S. M. (2003) African dust aerosols as atmospheric ice nuclei. *Geophys. Res. Lett.* **30**, 1732, doi:10.1029/2003GL017410.

Derbyshire E. (2003) Loess, and the Dust Indicators and Records of Terrestrial and Marine Palaeoenvironments (DIRTMAP) database. *Quat. Sci. Rev.* **22**, 1813–1819.

Derbyshire E. X. M. and Kemp R. A. (1998) Provenance, transport and characteristics of modern aeolian dust in western Gansu Province, China, and interpretation of the Quaternary loess record. *J. Arid Environ.* **39**, 497–516.

Ding Z. L., Sun J. M., Liu T. S., Zhu R. X., Yang S. L., and Guo B. (1998) Wind-blown origin of the Pliocene red clay formation in the central Loess Plateau, China. *Earth Planet. Sci. Lett.* **161**, 135–143.

Dubovik O., Holben B., Eck T., Smirnov A., Kaufman Y., King M., Tanre D., and Slutsker I. (2002) Variability of absorption and optical properties of key aerosol types observed in worldwide locations. *J. Atmos. Sci.* **59**, 590–608.

Dubovik O. and King M. (2000) A flexible inversion algorithm for retrieval of aerosol optical properties from Sun and sky radiance measurements. *J. Geophys. Res.—Atmos.* **105**, 20673–20696.

Duce R. A., Liss P. S., Merrill J. T., Atlas E. L., Buat-Menard P., Hicks B. B., Miller J. M., Prospero J. M., Arimoto R., Church T. M., Ellis W., Galloway J. N., Hansen L., Jickells T. D., Knap A. H., Reinhardt K. H., Schneider B., Soudine A., Tokos J. J., Tsunogai S., Wollast R., and Zhou M. (1991) The atmospheric input of trace species to the world ocean. *Global Biochem. Cycles* **5**, 193–259.

Eden D. N. and Hammond A. P. (2003) Dust accumulation in the New Zealand region since the last glacial maximum. *Quat. Sci. Rev.* **22**, 2037–2052.

Engelstaedter S., Kohfeld K. E., Tegen I., and Harrison S. P. (2003) Controls of dust emissions by vegetation and topographic depressions: an evaluation using dust storm frequency data. *Geophys. Res. Lett.* **30**, 1294, doi:10.1029/2002GL016471.

Frechen M., Oches E. A., and Kohfeld K. E. (2003) Loess in Europe—mass accumulation rates during the Last Glacial Period. *Quat. Sci. Rev.* **22**, 1835–1857.

Gardner W. D., Biscaye P. E., and Richardson M. J. (1997) A sediment trap experiment in the Vema Channel to evaluate the effect of horizontal particle fluxes on measured vertical fluxes. *J. Marine Res.* **55**, 995–1028.

Gill T. E., Gillette D. A., Niemeyer T., and Winn R. T. (2002) Elemental geochemistry of wind-erodible playa sediments, Owens Lake, California. *Nuclear Instruments and Methods in Physics Research Section B—Beam Interactions with Materials and Atoms* **189**, 209–213.

Gillette D. A. (1979) Environmental factors affecting dust emission by wind erosion. In *Saharan Dust* (ed. C. Morales). Wiley, New York, pp. 71–94.

Gillette D. A. (1999) A qualitative geophysical explanation for "hot spot" dust emitting source regions. *Contrib. Atmos. Phys.* **72**, 67–77.

Gillette D. A., Bifford I. H., Jr., and Fryrear, D. W. (1974) The influence of wind velocity on the size distribution of aerosols generated by the wind erosion of soils. *J. Geophys. Res.* **79**, 4068–4075.

Ginoux P., Chin M., Tegen I., Prospero J., Holben B., Dubovik O., and Lin S.-J. (2001) Global simulation of dust in the troposphere: model description and assessment. *J. Geophys. Res.—Atmos.* **106**, 20255–20273.

Ginoux P., Prospero J. M., Torres O., and Chin M. (2004) Long-term simulation of global dust distribution with the GOCART model: correlation with North Atlantic Oscillation. *Environ. Model. Software* **19**, 113–128.

Givelet N., Roos-Barraclough F., Goodsite M. E., Cheburkin A. K., and Shotyk W. (2004) Atmospheric mercury accumulation rates between 5900 and 800 calibrated years BP in the high Artic of Canada recorded by peat hummocks. *Environ. Sci. Technol.* **38**, 4964–4972.

Goudie A. S. and Middleton N. J. (1992) The changing frequency of dust storms through time. *Clim. Change* **20**, 197–225.

Grini A., Myhre G., Zender C., and Isaksen I. (2005) Model simulations of dust sources and transport in the global atmosphere: effects of soil erodibility and wind speed variability. *J. Geophys. Res.—Atmos.* **110**, Art. No. D02205.

Grini A. and Zender C. S. (2004) Roles of saltation, sandblasting, and wind speed variability on mineral dust aerosol size distribution during the Puerto Rican Dust Experiment (PRIDE). *J. Geophys. Res.—Atmos.* **109**, Art. No. D07202.

Grousset F. and Biscaye P. E. (2005) Tracing dust sources and transport patterns using Sr, Nd, and Pb isotopes. *Chem. Geol.* **222**, 149–167.

Grousset F. E., Ginoux P., Bory A., and Biscaye P. E. (2003) Case study of a Chinese dust plume reaching the French Alps. *Geophys. Res. Lett.* **30**, 1277.

Grousset F. E., Parra M., Bory A., Martinez P., Bertrand P., Shimmield G., and Ellam R. M. (1998) Saharan wind regimes traced by Sr–Nd isotopic composition of subtropical Atlantic sediments: last Glacial Maximum vs. today. *Quat. Sci. Rev.* **17**, 395–409.

Guo B., Zhu R. X., Roberts A. P., and Florindo F. (2001) Lack of correlation between paleoprecipitation and magnetic susceptibility of Chinese loess/paleosol sequences. *Geophys. Res. Lett.* **28**, 4259–4262.

Harrison S. P. and Prentice A. I. (2003) Climate and CO_2 controls on global vegetation distribution at the last glacial maximum: analysis based on palaeovegetation data, biome modelling and palaeoclimate simulations. *Global Change Biol.* **9**, 983–1004.

Haywood J., Allan R., Culverwell I., Slingo T., Milton S., Edwards J., and Clerbaux N. (2005) Can desert dust explain the outgoing longwave radiation anomaly over the Sahara during July 2003? *J. Geophys. Res.—Atmos.* **110**, D05105.

Haywood J., Francis P., Dubovik O., Glew M., and Holben B. (2003a) Comparison of aerosol size distributions, radiative properties, and optical depths determined by aircraft observations and Sun photometers during SAFARI 2000. *J. Geophys. Res.—Atmos.* **108**, 8471.

Haywood J., Francis P., Osborne S., Glew M., Loeb N., Highwood E., Tanre D., Myhre G., Formenti P., and Hirst E. (2003b) Radiative properties and direct radiative effect of Saharan dust measured by the C-130 aircraft during SHADE. 1: Solar spectrum. *J. Geophys. Res.—Atmos.* **108**, 8577.

Hermann J. R., Bhartia P. K., Torres O., Hsu C., Seftor C., and Celarier E. (1997) Global distribution of UV-absorbing aerosols from Nimbus 7/TOMS data. *J. Geophys. Res.—Atmos.* **102**, 16911–16922.

Hesse P. P. (1994) The record of continental dust from Australia in Tasman Sea sediments. *Quat. Sci. Rev.* **13**, 257–272.

Hesse P. P. and McTainsh G. H. (1999) Last Glacial Maximum to early Holocene wind strength in the mid-latitudes of the Southern Hemisphere from aeolian dust in the Tasman Sea. *Quat. Res.* **52**, 343–349.

Hesse P. P. and McTainsh G. H. (2003) Australian dust deposits: modern processes and the Quaternary record. *Quat. Sci. Rev.* **22**, 2007–2035.

Holben B., Eck T., Slutsker I., Tanre D., Buis J., Setzer A., Vermote E., Reagan J., Kaufman Y., Nakajima T., Lavenu F., Jankowiak I., and Smirnov A. (1998) AERONET—a federated instrument network and data archive for aerosol characterization. *Remote Sensing Environ.* **66**, 1–16.

Honjo S., François R., Manganini S. J., Dymond J., and Collier R. (2000) Particle fluxes to the interior of the Southern Ocean in the Western Pacific sector along 170° W. *Deep-Sea Res. II* **47**, 3521–3548.

Houghton J., Ding Y., Griggs D. J., Noguer M., van der Linden P. J., Dai X., Maskell K., and Johnson C. A. (2001) *Climate Change 2001: The Scientific Basis. Contribution of Working Group I to the Third Assessment Report of the Intergovernmental Panel on Climate Change*. Cambridge University Press, Cambridge, UK; New York, USA.

House J. I., Brovkin V., Betts R., Constanza R., Silva Dias M. A., Holland E., Que′re′ C. l., Kim Phat N., Riebesell U., and Scholes M. (2006) Air quality and climate, chapter 13. In *Ecosystems & Human Well-Being: Volume 1 Current States and Trends* (eds. R. Hassan, R. Scholes, and N. Ash). Island Press, Washington.

Iversen J. D. and White B. R. (1982) Saltation threshold on Earth, Mars, and Venus. *Sedimentology* **29**, 111–119.

Jickells T. D., An Z. S., Andersen K. K., Baker A. R., Bergametti G., Brooks N., Cao J. J., Boyd P. W., Duce R. A., Hunter K. A., Kawahata H., Kubilay N., laRoche J., Liss P. S., Mahowald N., Prospero J. M., Ridgwell A. J., Tegen I., and Torres R. (2005) Global iron connections between desert dust, ocean biogeochemistry, and climate. *Science* **308**, 67–71.

Johnson L. R. (1979) Particle size fractionation of eolian dusts during transport and sampling. *Marine Geol.* **21**, M17–M21.

Kahn R. A., Gaitley B. J., Martonchik J. V., Diner D. J., Crean K. A., and Holben B. (2005) Multiangle Imaging Spectroradiometer (MISR) global aerosol optical depth validation based on 2 years of coincident Aerosol Robotic Network (AERONET) observations. *J. Geophys. Res.—Atmos.* **110**, doi:10.1029/2004JD004706.

Kawahata H., Ohkushi K. I., and Hatakeyama Y. (1999) Comparative Late Pleistocene paleoceanographic changes in the mid latitude Boreal and Austral Western Pacific. *J. Oceanogr.* **55**, 747–761.

Kawahata H., Okamoto T., Matsumoto E., and Ujiie H. (2000) Fluctuations of eolian flux and ocean productivity in the mid-latitude North Pacific during the last 200 kyr. *Quat. Sci. Rev.* **19**, 1279–1292.

Kohfeld K. E. and Harrison S. P. (2001) DIRTMAP: the geologic record of dust. *Earth Sci. Rev.* **54**, 81–114.

Kohfeld K. E. and Harrison S. P. (2003) Glacial-interglacial changes in dust deposition on the Chinese Loess Plateau. *Quat. Sci. Rev.* **22**, 1859–1878.

Kohfeld K. E., Le Quéré C., Harrison S. P., and Anderson R. F. (2005) Role of marine biology in glacial-interglacial CO_2 cycles. *Science* **308**, 74–78.

Kurtz A. C., Derry L. A., and Chadwick O. A. (2001) Accretion of Asian dust to Hawaiian soils: isotopic, elemental, and mineral mass balances. *Geochim. Cosmochem. Acta* **65**, 1971–1983.

Laurent B., Marticorena B., Bergametti G., Chazette P., Maignan F., and Schmechtig C. (2005) Simulation of the mineral dust emission frequencies from desert areas of China and Mongolia using an aerodynamic roughness length map derived from the POLDER/ADEOS 1 surface products. *J. Geophys. Res.—Atmos.* **110**, Art. No. D18S04.

Levin Z., Teller A., Ganor E., and Yin Y. (2005) On the interactions of mineral dust, sea-salt particles, and clouds: a measurement and modeling study from the Mediterranean Israeli Dust Experiment campaign. *J. Geophys. Res.—Atmos.* **110**, D20202.

Liao H. and Seinfeld J. H. (1998) Radiative forcing by mineral dust aerosols: sensitivity to key variables. *J. Geophys. Res.—Atmos.* **103**, 31637–31645.

Lu H. and Shao Y. P. (1999) A new model for dust emission by saltation bombardment. *J. Geophys. Res.—Atmos.* **104**, 16827–16841.

Mahowald N., Kohfeld K. E., Hansson M., Balkanski Y., Harrison S. P., Prentice I. C., Schulz M., and Rodhe H. (1999) Dust sources and deposition during the Last Glacial Maximum and current climate: a comparison of model results with palaeodata from ice cores and marine sediments. *J. Geophys. Res.—Atmos.* **104**, 15895–15916.

Mahowald N. M., Baker A. R., Bergametti G., Brooks N., Duce R. A., Jickells T. D., Kubilay N., Prospero J. M., and Tegen I. (2005) Atmospheric global dust cycle and iron inputs to the ocean. *Global Biogeochem. Cycles* **19**, GB4025, doi:10.1029/2004GB002402.

Mahowald N. M. and Luo C. (2003) A less dusty future? *Geophys. Res. Lett*. **30**, 1903, doi:1910.1029/2003 GL017880.

Mahowald N. M., Muhs D. R., Levis S., Rasch P. J., Yoshioka M., Zender C. S., and Luo C. (2006) Change in atmospheric mineral aerosols in response to climate: last glacial period pre-industrial, modern and doubled carbon dioxide climates. *J. Geophys. Res.—Atmos.* **111**, D10202, doi:10.1029/2005JD006653.

Mahowald N. M., Rivera G. D. R., and Luo C. (2004) Comment on "Relative importance of climate and land use in determining present and future global soil dust emission" by I. Tegen *et al. Geophys. Res. Lett.* **31**, doi:10.1029/2004GL021272.

Mahowald N. M., Yoshioka M., Collins W. D., Conley A. J., Filmore D. W., and Coleman D. B. Climate response and radiative forcing from mineral aerosols during the last glacial maximum, pre-industrial, current and doubled-carbon dioxide climates. *Geophys. Res. Lett*. (in press).

Malm W., Schichtel B., Pitchford M., Ashbaugh L., and Eldred R. (2004) Spatial and monthly trends in speciated fine particle concentration in the United States. *J. Geophys. Res.—Atmos.* **109**, Art. No. D03306.

Marticorena B. and Bergametti G. (1995) Modeling the atmospheric dust cycle, 1, Design of a soil-derived dust emission scheme. *J. Geophys. Res.—Atmos.* **100**(D8), 16415–16430.

Martin J. (1990) Glacial-interglacial CO_2 change: the iron hypothesis. *Paleoceanography* **5**, 1–13.

Martin J. H. and Fitzwater S. E. (1988) Iron deficiency limits phytoplankton growth in the north-east Pacific subarctic. *Nature* **331**, 341–343.

Mbourou G. N., Bertrand J. J., and Nicholson S. E. (1997) The diurnal and seasonal cycles of wind-borne dust over Africa north of the equator. *J. Appl. Meteorol.* **36**, 868–882.

McTainsh G. H., Lynch A. W., and Tews E. K. (1998) Climatic controls upon dust storm occurrence in eastern Australia. *J. Arid Environ.* **39**, 457–466.

Middleton N. J. (1984) Dust storms in Australia: frequency, distribution and seasonality. *Search* **15**, 46–47.

Middleton N. J. (1986a) Dust storms in the Middle East. *J. Arid Environ.* **10**, 83–96.

Middleton N. J. (1986b) A geography of dust storms in south-west Asia. *J. Clim.* **6**, 183–196.

Miller R., Perlwitz J., and Tegen I. (2004) Feedback upon dust emission by dust radiative forcing through the planetary boundary layer. *J. Geophys. Res.—Atmos.* **109,** Art. No. D24209.

Moulin C. and Chiapello I. (2004) Evidence of the control of summer atmospheric transport of African dust over the Atlantic by Sahel sources from TOMS satellites (1979–2000). *Geophys. Res. Lett.* **31**, L02107, doi:10.1029/2003GL018931.

Moulin C., Lambert C. E., Dulac F., and Dayan U. (1997) Control of atmospheric export of dust from North Africa by the North Atlantic Oscillation. *Nature* **387**, 691–694.

Muhs D. R., Ager T. A., Bettis E. A., III, McGeehin J., Been J. M., Begét J. E., Pavich M. J., Stafford T. W., Jr., and Stevens D. A. S. P. (2003) Stratigraphy and palaeoclimatic significance of late quaternary loess–palaeosol sequences of the last interglacial–glacial cycle in central Alaska. *Quat. Sci. Rev.* **22**, 1947–1986.

Muhs D. R., Aleinikoff J. N., Stafford T. W., Jr., Kihl R., Been J., and Mahan S. A. (1999) Late Quaternary loess in northeastern Colorado. I: Age and paleoclimatic significance. *Geolog. Soc. Am. Bull.* **111**, 1861–1875.

Muhs D. R. and Benedict J. B. (2006) Eolian Additions to Late Quaternary Alpine Soils, Indian Peaks Wilderness Area, Colorado Front Range. *Arctic, Antarct., Alpine Res.* **38**, 120–130.

Muhs D. R. and Bettis E. A., III (2000) Geochemical variations in Peoria Loess of western Iowa indicate paleowinds of midcontinental North America during last glaciation. *Quat. Res.* **53**, 49–61.

Muhs D. R. and Bettis E. A., III (2003) Quaternary loess-paleosol sequences as examples of climate-driven sedimentary extremes. In *Extreme Depositional Environments: Mega End Members in Geologic Time* (eds. M. A. Chan and A. W. Archer), Geological Society of America Special Paper 370. Boulder, CO, pp. 53–74.

Muhs D. R., Bush C. A., Stewart K. C., Rowland T. R., and Crittenden R. C. (1990) Geochemical evidence of Saharan dust parent material for soils developed on Quaternary limestones of Caribbean and western Atlantic Islands. *Quat. Res.* **33**, 157–177.

National Climatic Data Center, http://www4.ncdc.noaa.gov/ol/documentlibrary/datasets.html (accessed June 2, 2006).

Nordstrom K. F. and Hotta S. (2004) Wind erosion from cropland in the USA: a review of problems, solutions and prospects. *Geoderma* **121**, 157–167.

Okin G. S. and Reheis M. C. (2002) An ENSO predictor of dust emission in the southwestern United States. *Geophys. Res. Lett.* **29**, doi:10.1029/2001GL014494.

Overpeck J., Rind D., Lacis A., and Healy R. (1996) Possible role of dust-induced regional warming in abrupt climate change during the last glacial period. *Nature* **384**, 447–449.

Parekh P., Dutkiewicz S., Follows M. J., and Ito T. (2006) Atmospheric carbon dioxide in a less dusty world. *Geophys. Res. Lett.* **33**, L03610.

Peltier W. R. and Marshall S. (1995) Coupled energy-balance/ice-sheet model simulations of the glacial cycle: a possible connection between terminations and terrigenous dust. *J. Geophys. Res.* **100**, 14269–14289.

Perlwitz J., Tegen I., and Miller R. (2001) Interactive soil dust aerosol model in the GISS GCM 1. Sensitivity of the soil dust cycle to radiative properties of soil dust aerosols. *J. Geophys. Res.—Atmos.* **106**, 18167–18192.

Petit J. R., Briat M., and Royer A. (1981) Ice age aerosol content from East Antarctic ice core samples and past wind strength. *Nature* **293**, 391–394.

Petit J. R., Jouzel J., Raynaud D., Barkov N. I., Barnola J. M., Basile I., Bender M., Chappellaz J., Davis M., Delaygue G., Delmotte M., Kotlyakov V. M., Legrand M., Lipenkov V. Y., Lorius C., Pepin L., Ritz C., Saltzman E., and Stievenard M. (1999) Climate and atmospheric history of the past 420,000 years from the Vostok ice core, Antarctica. *Nature* **399**, 436–439.

Pettke T., Halliday A. N., Hall C. M., and Rea D. K. (2000) Dust production and deposition in Asia and the north Pacific Ocean over the past 12 Myr. *Earth Planet. Sci. Lett.* **178**, 397–413.

Prigent C., Tegen I., Aires F., Marticorena B., and Zribi M. (2005) Estimation of the aerodynamic roughness length in arid and semi-arid regions over the globe with the ERS scatterometer. *J. Geophys. Res.—Atmos.* **110**, Art. No. D09205.

Prospero J. M. (1996) The atmospheric transport of particles to the ocean. In *Particle Flux in the Ocean* (eds. V. Ittekot, P. Schaefer, S. Honjo, and P. J. Depetris). Wiley, London, pp. 19–56.

Prospero J. M., Ginoux P., Torres O., Nicholson S. E., and Gill T. E. (2002) Environmental characterization of global sources of atmospheric soil dust identified with the Nimbus 7 Total Ozone Mapping Spectrometer (TOMS) absorbing aerosol product. *Rev. Geophys.* **40**, Art. No. 1002.

Prospero J. M. and Lamb P. J. (2003) African droughts and dust transport to the Caribbean: climate change implications. *Science* **302**, 1024–1027.

Pye K. (1987) *Aeolian Dust and Dust Deposits*. Academic Press, San Diego.

Pye K. (1995) The nature, orgin and accumulation of loess. *Quat. Sci. Rev.* **14**, 653–667.

Qiang X. K., Li Z. X., Powell C., and Zheng H. (2001) Magnetostratigraphic record of the Late Miocene onset of the East Asian monsoon, and Pliocene uplift of northern Tibet. *Earth Planet. Sci. Lett.* **187**, 83–93.

Rea D. K. (1994) The paleoclimatic record provided by eolian deposition in the deep sea: the geologic history of wind. *Rev. Geophys.* **32**, 159–195.

Reader M. C., Fung I., and McFarlane N. (2000) Mineral aerosols: a comparison of the last glacial maximum and preindustrial Holocene. *Can. J. Earth Sci.* **37**, 751–767.

Reheis M. and Kihl R. (1995) Dust deposition in southern Nevada and California, 1984–1989: relationship to climate, source area, and source lithology. *J. Geophys. Res.—Atmos.* **100**, 8893–8918.

Reheis M. C. (2003) *Dust Deposition in Nevada, California, and Utah, 1984–2002*, http://pubs.usgs.gov/of/2003/ofr-03-138/ (accessed 2006). U.S. Geol. Survey Open-File Report 03-138, Denver, CO.

Reheis M. C., Budahn J. R., and Lamothe P. J. (2002) Geochemical evidence for diversity of dust sources in the southwestern United States. *Geochim. Cosmochim. Acta* **66**, 1569–1587.

Reynolds R., Neff J., Reheis M., and Lamothe P. (2006) Atmospheric dust in modern soil on aeolian sandstone, Colorado Plateau (USA): variation with landscape position and contribution to potential plant nutrients. *Geoderma* **130**, 108–123.

Ridgwell A. and Kohfeld K. E. Dust in the Earth system: the biogeochemical linking of land, air, and sea. In *Advances in Science* (ed. P. Sammonds). Imperial College Press, London (in press).

Ridgwell A. J., Maslin M. A., and Watson A. J. (2002) Reduced effectiveness of terrestrial carbon sequestration due to an antagonistic response of ocean productivity. *Geophys. Res. Lett.* **29**, doi:10.1029/2001 GL014304.

Ridgwell A. J. and Watson A. J. (2002) Feedback between aeolian dust, climate, and atmospheric CO_2 in glacial time. *Paleoceanography* **17**, doi:10.1029/2001PA000729.

Roberts H. M., Muhs D. R., Wintle A. G., Duller G. A. T., and Bettis E. A., III (2003) Unprecedented last-glacial mass accumulation rates determined by luminescence dating of loess from western Nebraska. *Quat. Res.* **59**, 411–419.

Rosenfeld D., Rudich Y., and Lahav R. (2001) Desert dust suppressing precipitation: a possible desertification feedback loop. *Proc. Natl. Acad. Sci. USA* **98**, 5975–5980.

Ruddiman W. F. (1997) Tropical Atlantic terrigenous fluxes since 25,000 yrs B.P. *Marine Geol.* **136**, 189–207.

Schneider S. (2002) *Berichte-Fachbereich Geowissenschaften Universität Bremen*. Universität Bremen, Bremen, pp. 134.

Seinfeld J., Carmichael G., Arimoto R., Conant W., Brechtel F., Bates T., Cahill T., Clarke A., Doherty S., Flatau P., Huebert B., Kim J., Markowicz K., Quinn P., Russell L., Russell P., Shimizu A., Shinozuka Y., Song C., Tang Y., Uno I., Vogelmann A., Weber R., Woo J., and Zhang X. (2004) ACE-ASIA—regional climatic and atmospheric chemical effects of Asian dust and pollution. *Bull. Am. Meteorol. Soc.* **85**, 367.

Seinfeld J. A. and Pandis S. N. (1997) *Atmospheric Chemistry and Physics: From Air Pollution to Climate Change*. Wiley, New York.

Siegel D. A. and Armstrong R. A. (2002) Corrigendum to "Trajectories of sinking particles in the Sargasso Sea: modeling of statistical funnels above deep-ocean sediment traps" [*Deep-Sea Res. I* 44, 1519–1541]. *Deep-Sea Res. I* **49**, 1115–1116.

Siegel D. A. and Deuser W. G. (1997) Trajectories of sinking particles in the Sargasso Sea: modeling of statistical funnels above deep-ocean sediment traps. *Deep-Sea Res. I* **44**, 1519–1541.

Smalley I. J. and Krinsley D. H. (1978) Loess deposits associated with deserts. *Catena* **5**, 53–66.

Smalley I. J. and Smalley V. (1983) Loess material and loess deposits: formation distribution and consequences. In *Eolian Sediments and Processes* (eds. M. E. Brookfield and T. S. Ahlbrandt), Developments in Sedimentology. Elsevier, Amsterdam, pp. 51–68.

Sokolik I., Winker D., Bergametti G., Gillette D., Carmichael G., Kaufman Y., Gomes L., Schuetz L., and Penner J. (2001) Introduction to special section: outstanding problems in quantifying the radiative impacts of mineral dust. *J. Geophys. Res.—Atmos.* **106**, 18015–18027.

Steffensen J. P. (1997) The size distribution of microparticles from selected segments of the Greenland Ice Core Project ice core representing different climatic periods. *J. Geophys. Res.—Atmos.* **102**, 26755–26763.

Sun J., Kohfeld K. E., and Harrison S. P. (2000) *Records of aeolian dust deposition on the Chinese Loess Plateau during the Late Quaternary*. Max Planck Institute for Biogeochemistry, Jena, Germany, pp. 318.

Sun Y. B. and An Z. S. (2005) Late Pliocene-Pleistocene changes in mass accumulation rates of eolian deposits on the central Chinese Loess Plateau. *J. Geophys. Res.—Atmos.* **110**, doi:10.1029/2005JD006064.

Svensson A., Biscaye P. E., and Grousset F. E. (2000) Characterization of late glacial continental dust in the Greenland Ice Core Project ice core. *J. Geophys. Res.—Atmos.* **105**, 4637–4656.

Swap R., Garstang M., Greco S., Talbot R., and Kallberg P. (1992) Saharan dust in the Amazon Basin. *Tellus, Series-B* **l44B**, 133–149.

Tegen I. (2003) Modeling the mineral dust aerosol cycle in the climate system. *Quat. Sci. Rev.* **22**, 1821–1834.

Tegen I., Harrison S., Kohfeld K., Prentice I., Coe M., and Heimann M. (2002) Impact of vegetation and preferential source areas on the dust aerosol cycle. *J. Geophys. Res.—Atmos.* **107**, 4576, doi:10.1029/2001JD000963.

Tegen I., Lacis A., and Fung I. (1996) The influence on climate forcing of mineral aerosols from disturbed soils. *Nature* **380**, 419–422.

Tegen I., Werner M., Harrison S. P., and Kohfeld K. E. (2004a) Relative importance of climate and land use in determining present and future global soil dust emission. *Geophys. Res. Lett.* **31**, doi:10.1029/2003GL019216.

Tegen I., Werner M., Harrison S. P., and Kohfeld K. E. (2004b) Reply to comment by N. M. Mahowald *et al.* on "Relative importance of climate and land use in determining present and future global soil dust emission". *Geophys. Res. Lett.* **31**, doi:10.1029/2004GL021560.

Thompson L. G. (1977) Variations in microparticle concentration, size distribution and elemental composition fround in Camp Century, Greenland and Byrd station, Antarctica, deep ice cores. In *Proceedings of the Grenoble Symposium on Isotopes and Impurities in Snow and Ice*. IAHS-AISH, pp. 351–364.

Tiedemann R., Sarnthein M., and Shackleton N. J. (1994) Astronomic timescale for the Pliocene Atlantic $\delta^{18}O$ and dust flux records of Ocean Drilling Program site 659. *Paleoceanography* **9**, 619–638.

Tiessen H., Hauffe H. K., and Mermut A. R. (1991) Deposition of Harmattan dust and its influence on base saturation of soils in northern Ghana. *Geoderma* **49**, 285–299.

Visible Earth, http://visibleearth.nasa.gov (accessed 2006).

Vitousek P. M., Kennedy M. J., Derry L. A., and Chadwick O. A. (1999) Weathering versus atmospheric sources of strontium in ecosystems on young volcanic soils. *Oecologia* **121**, 255–259.

Washington R., Todd M., Lizcano G., Tegen I., Flamant C., Koren I., Ginoux P., Engelstaedter S., Bristow C., Zender C., Goudie A., Warren A., and Prospero J. (2006) Links between topography, wind, deflation, lakes and dust: the case of the Bodele Depression, Chad. *Geophys. Res. Lett.* **33**, L09401.

Watson A. J., Bakker D. C. E., Ridgwell A. J., Boyd P. W., and Law C. S. (2000) Effect of iron supply on Souther Ocean CO_2 uptake and implications for glacial atmospheric CO_2. *Nature* **407**, 730–734.

Werner M., Tegen I., Harrison S. P., Kohfeld K. E., Prentice I. C., Balkanski Y., Rodhe H., and Roelandt C. (2003) Seasonal and interannual variability of the mineral dust cycle under present and glacial climate conditions. *J. Geophys. Res.—Atmos.* **108**, doi:10.1029/2002JD002365.

Wheaton E. E. and Chakravarti A. K. (1990) Dust storms in the Canadian prairies. *Int. J. Climatol.* **10**, 829–837.

Woodward S., Roberts D. L., and Betts R. A. (2005) A simulation of the effect of climate change–induced desertification on mineral dust aerosol. *Geophys. Res. Lett.* **32**, doi:10.1029/2005GL023482.

Yu H., Kaufman Y., Chin M., Feingold G., Remer L., Anderson T., Balkanski Y., Bellouin N., Boucher O., Christopher S., DeCola P., Kahn R., Koch D., Loeb N., Reddy M., Schulz M., Takemura T., and Zhou M. (2006) A review of measurement-based assessments of the aerosol direct radiative effect and forcing. *Atmos. Chem. Phys.* **6**, 613–666.

Zárate M. A. (2003) Loess of southern South America. *Quat. Sci. Rev.* **22**, 1987–2006.

Zender C. S., Miller R. L., and Tegen I. (2004) Quantifying mineral dust mass budgets: terminology, constraints, and current estimates. *Eos* **85**, 509–512.

Zhao C., Dabu X., and Li Y. (2004) Relationship between climatic factors and dust storm frequency in Inner Mongolia of China. *Geophys. Res. Lett*. **31**, doi:10.1029/2003GL018351.

Zheng H. B., An Z. S., and Shaw J. (1992) New contributions to Chinese Plio-Pleistocene magnetostratigraphy. *Phys. Earth Planet. Interiors* **70**, 146–153.

Zheng H. B., Powell C. M., Rea D. K., Wang J., and Wang P. X. (2004) Late Miocene and mid-Pliocene enhancement of the East Asian monsoon as viewed from the land and sea. *Global Planet. Change* **41**, 147–155.

Zielinski G. A. and Mershon G. R. (1997) Paleoenvironmental implications of the insoluble microparticle record in the GISP2 (Greenland ice core during the rapidly changing climate of the Pleistocene–Holocene transition. *Geol. Soc. Am. Bull.* **109**, 547–559.

Treatise On Geochemistry
ISBN (set): 0-08-043751-6
pp. 1–26